

A simplified model for assessing lateral railway bridge resonance behavior

study on the lateral dynamics of railway bridges.

Sijian Deng

A thesis presented for the degree of
Master of Science



Faculty of Civil Engineering and Geo-science
Delft University of Technology Iv-Infra
The Netherlands
February 26, 2015 Iv-Groep

Abstract

Dynamics of railway bridges is a complicated problem that normally needs numerical simulation to conduct researches on. However, this thesis takes advantage of the numerical results provided in previous researches and based on these researches, further conclusions are made by using them in simplified model.

Recently long span railway bridges being designed in the Netherlands are being rejected by a particular Eurocode criterion that requires bridges to possess a first lateral natural frequency higher than 1.2Hz . Due to the fact that generally bridge's first lateral natural frequency decreases as the span increases, it can be seen that 1.2Hz criterion is rejecting almost all bridge with a span longer than 150m.

This report succeeds in pursuing the original documents of 1.2Hz criterion and the knowledge in the documents initiates further researches on the lateral dynamics of railway bridges. Besides 1.2Hz criterion itself, following topics are researched with the information provided by previous researches:

1. Train-bridge lateral resonance mechanisms, including axle repeat pattern resonance and kinematic movement resonance,
2. Lateral force on tracks caused by the operation of railway vehicle and key parameters influencing the force.

Taking advantage of the items above, a simplified model for checking the lateral railway bridge dynamics is developed to quantify the lateral dynamic resonance response of railway bridge under horizontal dynamic vehicle load. This method aims to serve for engineering purposes and provide an alternative way of verifying railway bridge lateral dynamics. The practical method is developed by an analytical approach, based on the numerical simulation results provided by other researches.

An illustration of the usage of the practical method is conducted on the basis of a real bridge project. The method is also implemented in Matlab scripts to automate the checking procedure.

Keywords:— Eurocode, railway bridge dynamics, lateral dynamics, rail dynamics, analytical solution, 1.2Hz criterion, train wavelength, nosing force, lateral force on track

Acknowledgments

Hereby I would like to express my deepest appreciation to all those who helped me in completing this thesis and my engineering studies.

First of all, I would like to thank to Matthijs van Almen, my daily supervisor at Iv-Infra, for his patient guidance during the entire thesis process. His guidance is like the light that helps me finding the right path in the darkness. Nevertheless, his way of thinking also enlightened me. I would never have completed the thesis without his help.

I also want to express my appreciation to Prof. Frans Bijaard, Ir. Roland Abspoel, Dr. Michaël Steenbergen, Prof. Rolf Dollevoet, the members of the thesis committee from Delft University of Technology. Their professional knowledge and general interest in the topic were valuable assets to my work.

Special thanks to Michel Koop, who provided me with the opportunity to carry out this research at Iv-Infra, to Charalampos Bouras, who was always eager to provide help whenever I needed, and to all the colleagues at the steel department of Iv-Infra, who provided me a friendly atmosphere.

I really appreciate the help of Ron van der Zwan and the access to ERRI D181 research resources he provided. I also appreciate Paul Vos, Jean-Jacques Reber sharing their background information of D181 committee. Same appreciation goes to Alan Minnis from DeltaRail for providing the information of D181 DT329 researches.

I am deeply grateful to my parents, Guolin Deng and Jiafen Wang, who always believed in me and were supporting my studies in The Netherlands.

Last but not least, I am thankful to all my friends in Delft, who gave me many unforgettable memories during my studies.

Sijian Deng

Delft, February 26, 2015

Contents

1	Introduction	8
1.1	Context of the thesis	8
1.2	Lateral dynamics of railway bridge	8
1.3	Objectives and research question	9
1.4	Main steps	9
1.5	Outline of the report	10
2	Theoretical background for lateral railway bridge dynamics	11
2.1	Wheel-rail interface	11
2.2	Lateral Track Irregularities	13
2.3	Lateral movement of wheelsets	14
2.4	Bridge natural frequency	16
2.5	Lateral vehicle-bridge resonance	16
3	Analysis of Eurocode criteria	18
3.1	Criterion based on bridge natural frequency	18
3.2	Criterion based on vehicle-induced lateral force	19
3.3	Conclusion	22
4	Methods for lateral dynamics assessment	23
4.1	Numerical methods	23
5	Simplified model for assessing lateral railway bridge resonance behavior	25
5.1	Assumptions	25
5.2	Equation of motion	26
5.3	The explicit solution	26
5.4	Mathematical validation of derived expressions	28
5.5	Parameter calculation	30
5.5.1	Peak lateral force model	31
5.5.2	Hypothesis expression for amplitude Q	34
5.6	Benchmark for the model	36
5.7	Supplementary parameter calculation and benchmark	39
5.8	Evaluation on the model	39

6 Practical usage of simplified model	41
6.1 Case study	41
6.2 Conclusion	43
7 Conclusion	44
8 Recommendations for future researches	46
8.1 Recommendations on numerical simulations	46
Appendices	48
A Literature Review of regulations regarding lateral railway bridge dynamics in 1991-2	49
A.1 Factors influencing dynamic behaviour	49
A.2 Requirements for railway bridge verification	50
A.3 Horizontal transverse dynamic effects	51
A.3.1 Nosing force	52
A.3.2 Verification of the Limit States	52
A.3.3 Serviceability limit states - traffic safety	53
A.3.3.1 Transverse deformations and vibrations	53
A.4 Conclusion	54
B General information of report series D181 and its selected documents	56
B.1 Structure of report series	56
B.2 Modelling of Parametric Research DT329	57
B.2.1 Model of bridge	57
B.2.2 Bridge parameters	57
B.2.3 Vehicle parameters	58
B.2.4 Track	59
B.2.5 Contact data	59
B.2.6 Data produced	59
C Plots and diagrams used in D181 DT 329	61
D Speeds which do not require dynamic compatibility checks	78
E MU-Groups and MU-Classes	82
E.1 Definition	82
E.1.1 Train parameters of MU-Class CB_1	83
E.1.2 Train parameters of MU-Class CB_2	83
E.1.3 Train parameters of MU-Class AB_1	83
E.1.4 Train parameters of MU-Class AB_2	83
E.1.5 Train parameters of MU-Class AB_3	83
E.1.6 Train parameters of MU-Class AB_4	83
E.1.7 Train parameters of MU-Class SA_1	83
E.1.8 Train parameters of MU-Class SA_2	83

F Regression commands for R console	86
G Matlab scripts	87
G.1 fog.m	87
G.2 Speedenvelop.m	90
H Train vehicles	92
H.1 Locomotives	92
H.1.1 4-axle locomotives	92
H.1.2 6-axle locomotives	92
H.2 Trains in Netherlands	92

List of Figures

2.1	Wheelset and track dimensions. Extracted from [9, p.17]	11
2.2	Coning of a wheel thread	12
2.3	Wheel profile S1002	13
2.4	Lateral track irregularity deviation definition[3]	13
2.5	Single and double contact of wheel-rail interface	14
2.6	Klingel movement. Extracted from [9, Figure 2.3]	15
2.7	Influence of flanging on lateral wheelset movement. Extracted from [9, Figure 2.5]	16
3.1	Figure C9 extracted from D181Committee [8]	21
4.1	A sample project being conducted in VAMPIRE	24
5.1	Schematic representation of a generic beam crossed by a harmonic load	26
5.2	Reference plot extracted from Abu-Hilal and Mohsen [2]. Condition: $\alpha = 0.25$, $\zeta = 0.05$, $\beta = 1$. Y axis for dynamic amplification factor.	29
5.3	Time history of dynamic amplification factor in mid-span of the beam. Parameters: $EJ = 2.43e10Nm^2$, $L = 54m$, $\mu = 6000kg/m$, $c = 29.26m/s$	30
5.4	Total peak lateral track forces over all track qualities(worn profile scenario neglected)	33
5.5	Figure C1 extracted from D181Committee [8]	35
5.6	Figure C3 extracted from D181Committee [8]	35
5.7	Figure C12 extracted from D181Committee [8]	36
5.8	Figure C13 extracted from D181Committee [8]	37
5.9	Figure C14 extracted from D181Committee [8]. An minor error is observed in y-axis label. Upper boundary of y-axis should be 0.116	37
5.10	Comparison between VAMPIRE peak simulation result and analytical peak result	38

6.1	Peak deflection at mid-span with regard to changing train speed. Parameters: $EJ = 6.56e12Nm^2$, $L = 255m$, $\mu = 20478kg/m$, $c_{min} = 1m/s$, $c_{max} = 30m/s$	42
B.1	Overview of modelling setups for different studies conducted in DT329	57
B.2	Bridge parameter combination	58
C.1	BR CLASS 56 LOCOMOTIVE. Extract from D181Committee [8, Appendix 2]	63
C.2	BR CLASS 56 LOCOMOTIVE. Extract from D181Committee [8, Appendix 2]	64
C.3	UIC FREIGHT WAGON (LADEN). Extract from D181Committee [8, Appendix 2]	65
C.4	UIC FREIGHT WAGON (LADEN). Extract from D181Committee [8, Appendix 2]	66
C.5	FS ETR500 LOCOMOTIVE. Extract from D181Committee [8, Appendix 2]	67
C.6	FS ETR500 LOCOMOTIVE. Extract from D181Committee [8, Appendix 2]	68
C.7	FS ETR500 COACH. Extract from D181Committee [8, Appendix 2]	69
C.8	FS ETR500 COACH. Extract from D181Committee [8, Appendix 2]	70
C.9	FS E444 LOCOMOTIVE. Extract from D181Committee [8, Appendix 2]	71
C.10	FS E444 LOCOMOTIVE. Extract from D181Committee [8, Appendix 2]	72
C.11	UIC COACH. Extract from D181Committee [8, Appendix 2]	73
C.12	UIC COACH. Extract from D181Committee [8, Appendix 2]	74
C.13	Horizontal track irregularities for freight trains. Extract from D181Committee [7, Figure 2.1]	75
C.14	Horizontal track irregularities for standard passenger trains. Extract from D181Committee [7, Figure 2.1]	76
C.15	Horizontal track irregularities for high speed passenger train. Extract from D181Committee [7, Figure 2.1]	77
D.1	Speed limit (in km/h) in relationship Line Category/Locomotive Class and vehicle type. Extract from CEN [6, Appendix F]	79
D.2	LATERAL WHEEL AND AXLE FORCES FOR BRIDGES. Extract from D181Committee [7, Fig 3.1]	80
D.3	Example run file. Extracted from D181Committee [8].	81
E.1	Train parameters related to MU-Groups. Extracted from CEN [6, Annex C]	84

List of Tables

2.1	Lateral standard deviation[Extracted from 3, Table B.6]	14
5.1	Peak Lateral Track Force Over All Track Qualities. Extracted From D181Committee [8, Tab. B1]	31
5.2	Parameter inputs and magnitude of amplitude Q	35
5.3	Comparison of results of simulation output and analytical output using refined load model	38
5.4	Constant component of amplitude $Q(N)$ from all available setups	39
5.5	Benchmark of explicit solution results	39
A.1	Maximum horizontal rotation and maximum change of radius of curvature	54
C.1	Axle repeat patterns and typical frequencies. Extracted from D181Committee [8, Appendix C]	61
C.2	Kinematic wavelength ranges per vehicle, with BR P1 profiles. Extracted from D181Committee [8, Appendix C]	62
E.1	Relationship MU-groups - MU-classes	83
E.2	Explanation of train parameters. Extracted from CEN [6, Annex C]	83
E.3	Train parameters for conformity with MU-Class CB_1	84
E.4	Train parameters for conformity with MU-Class CB_2	84
E.5	Train parameters for conformity with MU-Class AB_1	85
E.6	Train parameters for conformity with MU-Class AB_2	85
E.7	Train parameters for conformity with MU-Class AB_3	85
E.8	Train parameters for conformity with MU-Class AB_4	85
E.9	Train parameters for conformity with MU-Class SA_1	85
E.10	Train parameters for conformity with MU-Class SA_2	85

Chapter 1

Introduction

1.1 Context of the thesis

This master thesis is initiated by Iv-Infra to assist the designing of a long-span railway bridge.

During the validation process of bridge lateral dynamics, the bridge could not meet the Eurocode standard, that all railway bridges should possess first lateral natural frequency higher than 1.2Hz . However, for long-span(longer than $100m$) bridges with adequate structural safety, they normally possess first lateral natural frequencies that are below 1.0Hz . It is costly and excessive wasting to increase their first lateral natural frequency to 1.2Hz . Moreover, for the current stage of the project, it is not possible to modify the design of the bridge. Thus increasing the natural frequency of the bridge to meet the criterion is not a valid solution.

Moreover, there is no further instruction to guide the design when bridge can not meet this particular criterion. With no option left within the codes, Iv-Infra seeks alternative assessment for the safety of lateral dynamics of the railway bridge by initiating this thesis.

1.2 Lateral dynamics of railway bridge

Lateral dynamics of railway bridge is an engineering topic that relates to both bridge structure and operating railway vehicles. Till now there is no record of bridge/vehicle failure due to lateral railway vehicle dynamic loading.

There are few researches done on this topic. European Rail Research Institute(ERRI), former International Union of Railways(UIC), had systematically

investigated this topic in 1994. Several criteria proposed by the investigation were adopted in Eurocode.

1.3 Objectives and research question

The main objective of this thesis is to help Iv-Infra to assess the lateral dynamics of railway bridge. In order to do so, the principle of assessing lateral dynamics must be comprehended first.

Eurocode has offered assessing methods in its criteria related to lateral dynamics of railway bridges. However, there's no additional explanation for these criteria. In other words, the principle of the assessing methods is uncertain. Thus, the first objective of this thesis is to analyze the criteria in Eurocode, in order to interpret the principle of Eurocode assessing methods. By using the principle interpreted in previous step, the development of an alternative assessing method can be inspired and guided.

As a conclusion, the objectives of this thesis can be summarized as follows:

- Analyze Eurocode criteria and interpret the principle of lateral dynamics assessing process
- Find an alternative method to assess the lateral dynamics of railway bridges

The research question can be summarized as:

Interpret the principle of lateral dynamics validation process and develop an alternative method to assess the lateral dynamics of railway bridges

1.4 Main steps

In order to carry out the objectives and research questions, the thesis project is planned to be conducted in following steps:

1. Literature research on the theory of lateral railway bridge dynamics
2. Filter out Eurocode criteria related to lateral dynamics of railway bridges and trace the origin of these criteria
3. Analyze these criteria and conclude the principle of Eurocode assessing method
4. Develop an alternative method for assessing the lateral dynamics of railway bridges

5. Use the alternative method to validate the bridge design of Iv-Infra

1.5 Outline of the report

The report consists of 3 main parts: **Introduction**, **Body** and **Conclusion**.

Introduction contains Context of the thesis, Brief introduction to the topic, Research objectives and question and Outline of the report.

Body is consisted of three parts. The first part contains literature research on the theory of lateral railway bridge dynamics. The second part mainly aims to describe the analysis process and the conclusion of the analysis while the third part aims to describe the development of the alternative assessing method.

Conclusion contains conclusions for the whole thesis and recommendations for whom may concern in the future.

Thus the outline can be concluded as follows:

1. Introduction

- a. Context of the thesis
- b. Brief introduction to the topic
- c. Research objectives and question
- d. Outline of the report

2. Body

- a. Literature research on the theory of lateral railway bridge dynamics
- b. Analysis of Eurocode criteria
- c. Development of alternative assessing method

3. Conclusion

- a. Conclusions
- b. Recommendations

Chapter 2

Theoretical background for lateral railway bridge dynamics

This chapter contains theoretical basis of lateral railway bridge dynamics. The lateral dynamics of railway bridge is related to both structural dynamics and railway vehicle dynamics. This chapter aims to elaborate the basic concepts of both dynamics topics.

The railway vehicle dynamics part contains knowledge of *Wheel-rail interface*, *Lateral track irregularities* and *Lateral movement of wheelsets*. The structural dynamics part will introduce knowledge about *Bridge natural frequency*.

A brief introduction to the resonant interaction between bridge and vehicle is described in *Lateral vehicle-bridge resonance*.

2.1 Wheel-rail interface

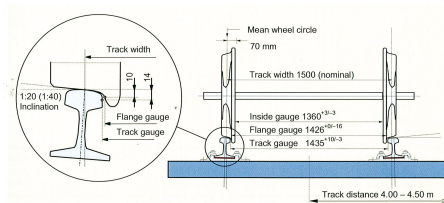


Figure 2.1: Wheelset and track dimensions. Extracted from [9, p.17]

Wheelset and track dimensions The dimensions of wheelset and track are regulated by International Union of Railways(UIC). Nowadays most of the Dutch rail uses *standard international dimension*. The bridge being designed by Iv-Infra will also apply standard rail dimensions.

The dimension of wheelset and track is explained in Figure.2.1.

Track gauge is defined as a distance between the two rails. On standard track the gauge is 1435^{+10}_{-3} mm with a maximum gradient of 1 : 3000. For new track, however, NS apply the following standards[9]:

1. Mean gauge per 200 m: 1435^{+10}_{-1} mm
2. Standard deviation within a 200 m section less than 1 mm

Conicity of wheels and equivalent conicity of wheels Conicity of wheels is an important factor influencing the lateral movement of wheelset. Conicity affects the dynamic behavior of wheelsets, therefore affecting the lateral dynamics of the railway vehicles.

The conicity is the inclination of a wheel thread section. Originally conical wheel thread profiles an inclination of 1:20 as shown in Figure.2.2.

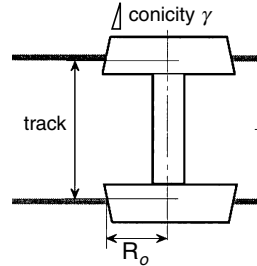


Figure 2.2: Coming of a wheel thread

However, during the manufacturing the tires are given a different shape from a straight conicity. The shape is hollow thus the straight conicity can not effectively describe the geometry of a actual wheel profile. For instance, the S1002 profile defined by UIC is shown in Figure.2.3.

Equivalent conicity is defined to describe the over-all inclination characteristics of a wheel profile. Generally, the equivalent conicity is defined as[9]:

$$\gamma_e = \frac{\Delta r}{2y} = \frac{r_1 - r_2}{2y}$$

$r_1 - r_2$ is the instantaneous difference in rolling radius of the wheel treads; generally speaking this is a non-linear function of the lateral displacement y of

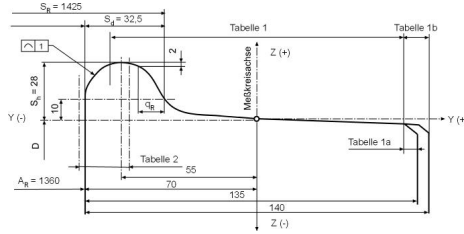


Figure 2.3: Wheel profile S1002

the wheelset with respect to the central position.

Worn wheel profiles Wheel wears during usage and wheel profiles will change under the effect of wear. Over a period of time wheel profiles stabilize with wear at an equivalent conicity of 0.2 to 0.3[9].

2.2 Lateral Track Irregularities

Lateral track irregularities is a source inducing the lateral movement of wheelsets. Track irregularities are minor track deformations that deviate from the original track reference. Well-maintained railway tracks have reduced lateral track irregularities and higher vehicle lateral stability.

The definition is shown in Figure 2.4. See Eurocode[3] for detailed information about the definition.

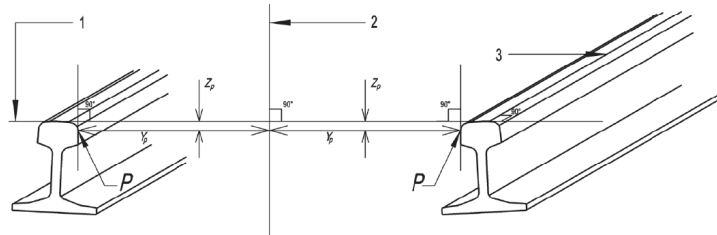


Figure 2.4: Lateral track irregularity deviation definition[3]

Table 2.1[3] defines the allowable standard deviation for lateral track irregularities.

Table 2.1: Lateral standard deviation [Extracted from 3, Table B.6]

Speed(km/h)	Standard deviation(mm)
$V \leq 90$	1.5 to 1.8
$80 < V \leq 120$	1.2 to 1.5
$120 < V \leq 160$	1.0 to 1.3
$160 < V \leq 230$	0.8 to 1.1
$230 < V \leq 300$	0.7 to 1.0

2.3 Lateral movement of wheelsets

Lateral movement of wheelsets is an essential topic to lateral dynamics of railway bridge because lateral loads on bridge are in direct consequence of lateral movement of wheelsets.

Contact between wheel and rail The movement characteristics of wheels depends on the contact type. There are two types of wheel-rail contact: single-point contact and two-point contact.

In the case of single-point contact, according to Figure 2.5a, wheel load and lateral force act on the same point. This situation occurs when using worn wheel profiles. In the case of two-point contact, shown in Figure 2.5b, the application points do not coincide.

Flanging occurs in the situation of two-point contact.

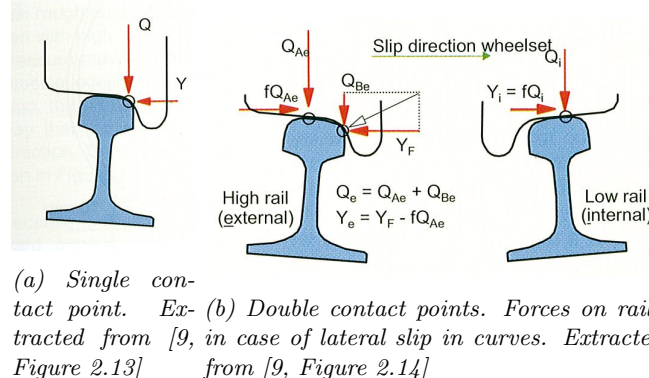


Figure 2.5: Single and double contact of wheel-rail interface

Klingel movement The Klingel movement happens under single-point contact.

Klingel described a periodical movement of the wheelset with conical tire profiles, which is also known as Klingel movement. It was assumed that the wheelset is laterally displaced from central position and the track is ideally straight. This displacement is expected to be counteracted due to different rolling radii of wheels.

Analysis visualizes the Klingel movement, shown in Figure 2.6. The lateral displacement y is a harmonic, undamped function of the distance co-ordinate x as long as the amplitude moves within the wheel flangeway clearance. However, it should be noted that forces play no part in the derivation. Thus Klingel movement is purely a kinematic movement.

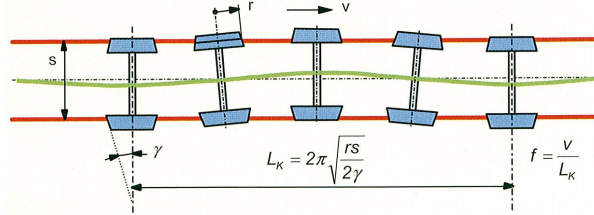


Figure 2.6: Klingel movement. Extracted from [9, Figure 2.3]

The expression for wavelength of Klingel movement is shown in Eq.2.1.

$$L_k = 2\pi \sqrt{\frac{rs}{2\gamma}} \quad (2.1)$$

where :

- | | |
|----------|--------------------------------|
| L_k | Wavelength of Klingel movement |
| r | Radius of wheels |
| s | Gauge distance |
| γ | Conicity of wheels |

Introducing the speed, the frequency of Klingel movement is Eq.2.2.

$$f = \frac{V}{L_k} \quad (2.2)$$

Hunting movement The hunting movement happens under two-point contact. Flanging happens in hunting movement.

It should be noted that the Klingel theory is simple and instructive but does not include the effect of coupled axes, mass forces, and adhesion forces. In reality, the amplitude y_0 of the Klingel movement is dependent on alignment, dynamic vehicle behavior, and the speed of the rolling stock.

Generally speaking, y_0 due to slip will increase with speed until it is equal to half the flangeway clearance. Flanging then occurs as a result of which the axle will rebound.

This means that the lateral movement takes on a completely different behavior which is known as hunting. As shown in the drawing in Figure 2.7 the movement changes from a harmonic to a zig-zag shape. The wavelength becomes shorter and the frequency increases quickly as hunting effect builds up.

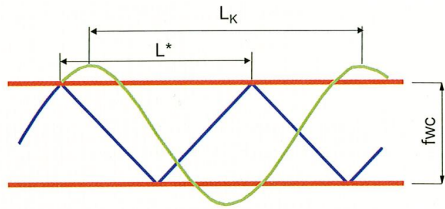


Figure 2.7: Influence of flanging on lateral wheelset movement. Extracted from [9, Figure 2.5]

2.4 Bridge natural frequency

The natural frequency of a bridge is an important characteristics of its structural dynamics.

Research[11] shows simplified method can be used to predict the natural frequencies of a bridge. The bridge is modeled as a uniform, simply supported beam. It is validated that the natural frequency of the beam approximately equals to the natural frequency of the bridge.

The beam is simply supported at both ends, and the stiffness of the beam is specified as a deflection at the mid span per unit span length arising from a static point load of 100kN at mid span on the bridge. The length of the beam equals to the span of the bridge. The total mass of the bridge is uniformly distributed over the beam.

The derived natural frequencies of the bridge is shown in Eq.2.3.

2.5 Lateral vehicle-bridge resonance

The resonance mechanism between railway vehicle and bridge is a complicated topic. Two types of vehicle-bridge resonance have been validated to be possible by UIC[8]. They are:

1. Resonance caused by axle repeat pattern

$$f_r = \frac{r^2\pi}{2L^2} \sqrt{\frac{EI}{m}} \quad (2.3)$$

where :

r	Natural mode:1,2,3...
L	Span of the bridge
EI	Equivalent stiffness of the bridge
m	Mass per unit length of the bridge

2. Resonance caused by kinematic movement

Resonance caused by axle repeat pattern Axle repeat pattern is the periodic pattern of train axles passing on a fixed location. The axle repeat pattern introduces forces to rail track on both vertical and lateral direction.

The wavelength of the axle repeat pattern is only dependent on the layout of the train. Although the distance between any two axles can form a wavelength, due to the regular arrangement coaches/wagons, there are only a few dominant wavelength.

Since frequency is speed divided by wavelength, the frequency of the axle repeat patterns vary with train speed. A table of axle repeat pattern lengths, and typical frequencies arising from train speed are given in Figure.C.1

Research[8, 3.4.3] shows that by running train at different speeds, resonance is possible between train and bridge if the axle passing frequency coincides with the first lateral bridge mode. The resonance effect is more pronounced compared to kinematic movement resonance[8, Chapter 5, Research Phase II].

Resonance caused by kinematic movement The lateral kinematic movement of railway vehicles is also wavelength phenomenon. However, the wavelength of lateral kinematic movement is much more complicated than axle repeat pattern. Many factors affect the wavelength of vehicle lateral kinematic movement. These factors include track irregularities, wheel profile, rail profile and other factors that may influence the lateral movement of wheelsets.

The lateral kinematic wavelength of railway vehicles are hard to predict. Research[8] obtains the lateral kinematic wavelength of the vehicle by numerical modeling a running railway vehicle.

The frequency of kinematic movement resonance is speed divided by wavelength. By coinciding the lateral kinematic frequency of the vehicle and bridge first lateral natural frequency, the resonance caused by kinematic movement was successfully validated[8].

Chapter 3

Analysis of Eurocode criteria

This chapter aims to analyze the Eurocode criteria that are related to lateral dynamics of railway bridges and discover their background principle. There are two types of criteria: bridge-natural frequency based criterion and vehicle-induced lateral force criterion.

It has been discovered that UIC research[7] is the original research that proposed both types of criteria.

3.1 Criterion based on bridge natural frequency

Criterion definition and background The bridge natural frequency based criterion is defined in [4, A24.4.2.4] by following statement:

...

The first natural frequency of lateral vibration of a span should not be less than f_{h0} . The value for f_{h0} may be defined in the National Annex. The recommended value is: $f_{h0} = 1.2\text{Hz}$

...

The original proposal can be found in [7, Proposed criteria]. The original intention of criterion is explained by following quote text:

To avoid the occurrence of resonance in the lateral motion of the vehicles due to the lateral motion of the bridge, a limit value lower than the first natural frequency f_{1t} of the lateral vibration of the span studied should be fixed. The natural frequency for lateral movements

is between 0.5 and 0.7 Hz for coaches and between 0.7 and 1 Hz for locomotives. We therefore propose a safety margin $F_{lt} \geq 1.2\text{Hz}$

Criterion principle From the original proposal, it can be concluded that this criterion intends to avoid the resonance between the vehicle and the bridge.

There is no additional explanation about what type of resonance is being avoided. The *natural frequency* in the original text is also unclear. There is no explanation on the natural frequency, either.

It can be concluded that the original text is referring to the natural frequency of an uncertain vibrating mode of the vehicle. The magnitude of the frequency in original proposal is independent of speed, thus it can be guessed that the frequency refers to the natural frequency of a typical rigid body mode of the vehicle. It may be the lateral swing mode of railway vehicles.

However, the resonance described in the original text does not belong to any resonance type validated in previous research. This is because resonance caused by both axle repeat pattern and kinematic movement happens at frequencies related to vehicle speed. There is no research supports the resonance theory described in this criterion.

As a conclusion, the criterion lacks theoretical support. No evidence proofs the resonance mentioned in the original text can happen. No background principle can be extracted from this criterion.

3.2 Criterion based on vehicle-induced lateral force

The criterion based on vehicle-induced lateral force is the global criterion governing the validation of structural safety. The criterion itself is generic and unrelated to the topic of lateral dynamics of railway bridge. To be more specific, this section aims to analyze the vehicle-induced lateral force which is a load input for the global criterion.

There are several types of vehicle-induced lateral force mention in Eurocode[4] but this thesis only concerns uniform motion and straight railway tracks. Thus one type of force, Nosing force, is selected and analyzed.

Definition and background of nosing force The nosing force is defined in [4, 6.5.2] with following statement:

- (1)P The nosing force shall be taken as a concentrated force acting horizontally, at the top of the rails, perpendicular to the centre-line of track. It shall be applied on both straight track and curved track.

(2)P The characteristic value of the nosing force shall be taken as $Q_{sk} = 100kN$. It shall not be multiplied by the factor Φ (see 6.4.5) or by the factor f in 6.5.1(4).

(3) The characteristic value of the nosing force in 6.5.2(2) should be multiplied by the factor α in accordance with 6.3.2(3) for values of $\alpha \geq 1$.

(4)P The nosing force shall always be combined with a vertical traffic load.

The background research[8] illustrates detailed information about nosing force. The research sets up different scenarios and simulates the scenarios in numerical modeling software. The peak total lateral forces on track are generated from these simulations. After that these peak lateral forces are used to generate the magnitude of the nosing force.

The research obtains peak lateral force by running simulations over a large range of track qualities and wheel conicity from 0.42 mm to 6.2 mm and 0.05 to 0.4 respectively. The track quality range represents a range from best quality high-speed line to poor quality freight track and would therefore be expected to cover the full range of track qualities likely to be found on a railway bridge. The conicity range represents that which can usually be expected to occur for trains running on conventional speed lines.

It has been verified that the peak lateral force on track is greatly affected by track irregularities and wheel conicity. In other words, the poorer the tracks and wheels are maintained, the greater the peak lateral force on track will be.

Analysis of nosing force From the definition of nosing force, it can be seen that nosing force is an imaginary concentrated force which does not represent the real lateral force distribution on track. It aims to represent the total peak lateral force magnitude generated by the whole vehicle.

For long-span railway bridges, the actual lateral force is axle forces distributed along the the span. Compared to concentrated nosing force, whose magnitude equals to the total sum of magnitude axle forces, the distributed axle force yields lower structural deformation. The nosing force is conservative compared to axle forces in terms of structural mechanics.

However, for nowadays Dutch railways, the wheels and tracks are maintained according to Eurocode regulations so the track irregularities and wheel conicity are well below the most unfavorable scenario simulated in UIC research. This means the peak lateral forces generated by these simulations are too high compared to real peak lateral forces on nowadays Dutch railway tracks. Thus for the same reason, the nosing force whose magnitude is determined using those simulation is too conservative.

Verification on nosing force magnitude Nosing force in Eurocode has characteristic value of 100kN, which is lower than the original proposed magnitude in its background research. Additional calculation is carried out to verify if the magnitude is sufficient.

The verification is done by comparing peak displacement caused by 100kN nosing force and peak displacement result of numerical simulation done on the same bridge. The numerical simulation is provided by UIC research[8].

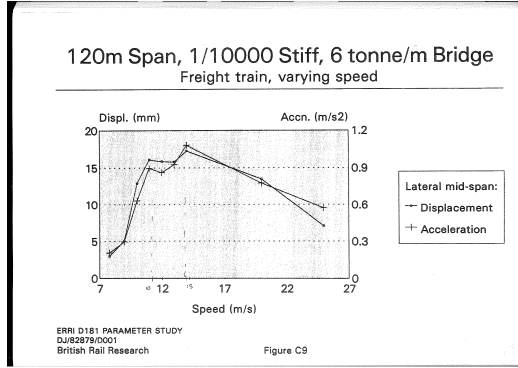


Figure 3.1: Figure C9 extracted from D181 Committee [8]

Figure 3.1 illustrates a chosen simulation case. The bridge possesses following parameters:

$$\begin{aligned} l &= 120m \\ Stiff^1 &: 1/10000 \\ \mu &= 6000kg/m \end{aligned}$$

Peak result for numerical simulation: 17mm

According to the definition, the characteristic value of the nosing force shall be taken as $Q_{sk} = 100kN$. It shall not be multiplied by the factor Φ or by the factor f . Thus, according to simple support Euler-beam theory, the deflection under 100kN nosing force is:

$$\delta_{nosing} = 120m \cdot 1/10000 = 0.012m = 12mm$$

It can be seen that nosing force does not give conservative result compared to numerical simulations. The reason for the nonconservative result is that this simulation case reproduced vehicle-bridge resonance so the peak displacement is amplified. It can be concluded that nosing force in Eurocode does not take resonance effects into account. It is nonconservative when resonance between vehicle and bridge happens.

¹deflection/span ratio at midspan under 100kN point load at midspan

3.3 Conclusion

According to the analysis, the Eurocode criterion based on bridge natural frequency lacks theoretical support thus no principle can be extracted from this criterion. The resonance type described in the criterion is not validated by any research and the criterion can not avoid any known resonance type.

The criterion based on lateral forces is feasible but too conservative in original proposal because nowadays tracks and wheels are well maintained so lateral forces on tracks are much smaller than those generated from UIC simulations. However, nosing force in Eurocode is reduced in magnitude due to unknown reasons and the reduction may result in nonconservative result when resonance happens.

Thus it can be concluded that Eurocode criteria on lateral dynamics of railway bridge lack adequate verification on resonance effects.

Since the bridge of Iv-Infra can not meet bridge natural frequency based criterion and this criterion is intended to solve resonance issues, the bridge should be verified for its lateral resonance behavior. Since the Eurocode criterion does not make sense, alternative assessment method for lateral railway bridge resonance behavior needs to be applied on the bridge of Iv-Infra.

Chapter 4

Methods for lateral dynamics assessment

Several analysing methods for vertical dynamics of railway bridges were briefed in UIC [12, A6.2]. Methods that can be applied also on lateral direction are selected:

...

Various programs such as ANSYS, NASTRAN, ABAQUS, SAP, FASTRUDL and so on, can be used to obtain the modal responses of bridge decks. Modeling can be done with beam models using torsional characteristics if the bridge is not a skew bridge and the structure is not a special case (see above). However, spatial modeling is necessary in such cases. ...

4.1 Numerical methods

When the analysis uses numerical methods to directly integrate the dynamic equation, the loads become the dynamic system in the case of vehicles and their internal behavior impacts the response from the structure.

- the two systems can be considered separate systems,
- the vehicle can be considered a finite element.

This last method takes track profile defects into account and deduces the force of interaction between the structure and the vehicle as well as the internal forces in the dynamic system that is built.

In this method, the equation of the dynamics is solved, with or without prior transformation, by using the conventional algorithms for numerical resolution of second-degree differential equations. These numerical methods calculates the response to regularly spaced time intervals(in general). The selected time pitch determines the accuracy of the results and has a bearing on the length of computer calculations.

Numerical integration methods are all based on the search for balanced solutions of the dynamic equation at regular time intervals.

VAMPIRE VAMPIRE is a FEM simulation software developed by DeltaRail. It allows the user to build a dynamic model of any rail vehicle and study the response of the vehicle to real measured track geometry or user specified inputs in the form of track displacements and external force inputs. Rail vehicles can be modeled with simulated instrumentation allowing almost any aspect of behavior to be studied.

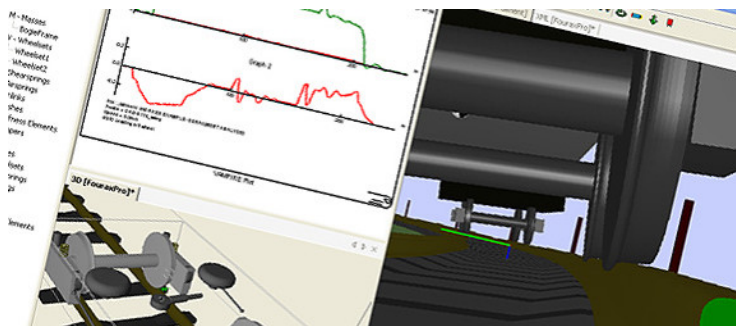


Figure 4.1: A sample project being conducted in VAMPIRE

There are also many similar simulation software on the market which puts emphasis on railway vehicle dynamic behavior, but VAMPIRE is specially selected for introduction because it was the software used by UIC committee, whose report series originally proposed 1.2Hz criterion by using the assistance of VAMPIRE. Also, the output results provided by UIC reports is an important foundation for the development of new practical method.

Chapter 5

Simplified model for assessing lateral railway bridge resonance behavior

This simplified model aims to simulate the lateral resonance behavior of a railway bridge.

5.1 Assumptions

It is assumed that the bridge is straight and uniform, simply supported on both ends. One track is installed on the center-line of the bridge. A train is moving uniformly along the track. The train and the bridge are under resonance. Only lateral displacement is taken into account. Deformations of other directions are neglected.

The bridge is modeled as a uniform, simply supported beam. The deflection of the beam represents the lateral deflection of the bridge. The stiffness of the beam is specified as a deflection at the mid span per unit span length arising from a static point load at mid span on the bridge. The length of the beam equals to the span of the bridge. The mass of the beam equals to the mass of the bridge.

A concentrated load presenting the total lateral force induced from the vehicle to the bridge is applied on the beam. The concentrated load is harmonically exciting the beam thus simulating the vehicle-bridge resonance.

The resonance is simulated by setting the magnitude of the concentrated load to oscillate under the same frequency as the first lateral natural frequency of

the bridge. The movement of the vehicle is also simulated by setting the load to move at a constant speed, from one end of the beam towards the other end of the beam.

The force initially locates at one end when time is 0. Force initial phase is 0.

The model diagram is presented Figure.5.1.

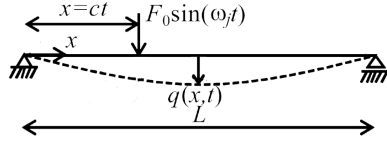


Figure 5.1: Schematic representation of a generic beam crossed by a harmonic load

5.2 Equation of motion

The governing equation motion for the model is shown in Eq.5.1.

$$EJ \frac{\partial^4 v(x, t)}{\partial x^4} + \mu \frac{\partial^2 v(x, t)}{\partial t^2} + 2\mu\omega_b \frac{\partial v(x, t)}{\partial t} = \delta(x - ct)Q \sin \Omega t \quad (5.1)$$

where :

EJ	Lateral stiffness of the beam
v	Lateral displacement of the beam
x	Horizontal axis label
μ	Mass per unit length of the beam
ω_b	Circular frequency of damping
c	Speed of moving load
Q	Amplitude of load
Ω	Circular frequency of load. Ω equals to first lateral natural frequency of the bridge
δ	Delt function

5.3 The explicit solution

The explicit solution of the motion equation is derived by Fryba[10]. Derived equation for mid-span lateral displacement is Eq.5.2. *This equation will be referred as 'the explicit solution' in following paragraphs.*

$$v(l/2, t) = \frac{l^3 Q \omega_{(1)}}{\pi^4 E J} \frac{\cos \omega_{(1)} t}{\omega^2 + \omega_b^2} [\omega(\cos \omega t - e^{-\omega_b t}) - \omega_b \sin \omega t] \quad (5.2)$$

where :

l	span of the beam(m)
ζ	damping ratio
ω_1	first natural circular frequency of the beam
	$= \frac{\pi^2}{l^2} \sqrt{\frac{EJ}{\mu}}$
ω	$= \pi c/l$
ω_b	$= \frac{1}{2} \zeta \omega_1$

Damping in the expression This paragraph aims to derive the correct expression for the damping component in the expression for Eq.5.2.

Eq.5.1 uses a form of damping expression ω_b , which can be converted from normal damping coefficient. Equation of motion using damping coefficient is shown in Eq.5.3:

$$EJ \frac{\partial^4 v(x, t)}{\partial x^4} + \mu \frac{\partial^2 v(x, t)}{\partial t^2} + \chi \frac{\partial v(x, t)}{\partial t} = \delta(x - ct) Q \sin \Omega t \quad (5.3)$$

where χ stands for damping coefficient. By comparing 5.3 and 5.1:

$$\omega_b = \frac{\chi}{2\mu} \quad (5.4)$$

where:

ω_b : circular frequency of damping

χ : damping coefficient

μ : mass per unit length of the bridge

also, in [2, Page.704] it is mentioned that:

The external and internal damping of the beam are assumed to be proportional to the mass and stiffness of the beam respectively,i.e.,
 $r_a = \gamma_1 \mu ..$, where γ_1 and γ_2 are proportionality constants.

thus:

$$\omega_b = \frac{\gamma_1}{2} \quad (5.5)$$

and it is mentioned in [2, Eq.8] that:

$$\zeta = \frac{\gamma_1}{\omega_1}$$

so:

$$\gamma_1 = \zeta \omega_1$$

so:

$$\omega_b = \frac{1}{2} \zeta \omega_1 = \frac{1}{2} \frac{\zeta \pi^2}{l^2} \sqrt{\frac{EJ}{\mu}}$$

5.4 Mathematical validation of derived expressions

Since circular frequency of damping ω_b is not clearly defined by Fryba, it is necessary to verify the correctness of both explicit solution and deduced ω_b expression.

The verification is done by comparing the result of Eq.5.2 with the result of a explicit solution in a different form obtained by another deducing method.

The result in Abu-Hilal and Mohsen [2] is selected to be the benchmark for verification. This report is researching vibration of beams with general boundary conditions due to a moving harmonic load. The differential equation is illustrated as follows:

$$EIv'''' + \mu \ddot{v} + r_a \dot{v} + r_i v''' = p(x, t) \quad (5.6)$$

The difference between Eq.5.6 and Eq.5.2 is that it offers broader boundary conditions such as changing speed of the load and various kinds of supports. As a result of more general equation, the deduction steps are much more complicated. However, two solutions should yield same results under same boundary conditions that:

1. Load moving at constant speed,
2. Frequency of load equals frequency of the beam,
3. Internal damping is 0,
4. Simple hinge support at both ends of the beam.

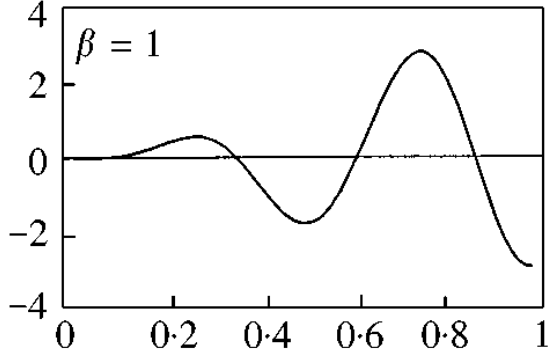


Figure 5.2: Reference plot extracted from Abu-Hilal and Mohsen [2]. Condition: $\alpha = 0.25$, $\zeta = 0.05$, $\beta = 1$. Y axis for dynamic amplification factor.

One plot from the parametric study of Abu-Hilal and Mohsen [2] meets the above requirement and is selected and illustrated in Figure. Parameters used in this plot is $\alpha = 0.25$, $\zeta = 0.05$, $\beta = 1$

Next step is to translate parameters used in above plot to usable parameters in Eq.5.2.

$$c_{cr} = \frac{\omega_1 L}{\pi} = \frac{\pi}{l} \sqrt{\frac{EJ}{\mu}}$$

$$c = \alpha c_{cr} = \frac{\alpha \pi}{l} \sqrt{\frac{EJ}{\mu}}$$

EJ, μ, l needs to be selected to yield value for c , thus following values are randomly selected:

$$\begin{aligned} EJ &= 2.43e10 Nm^2 \\ l &= 54m \\ \mu &= 6000 kg/m \\ c_{cr} &= 117.05 m/s \\ c &= 29.26 m/s \end{aligned}$$

A Matlab script is written to automate numerical calculating procedure. The script is presented in Appendix.G. By typing

```
>>fog(2.43e10,54,6000,29.26,0.05)
```

into the console. Figure.5.3 is obtained.

By observing Figure.5.2 and Figure.5.3 it can be concluded that results are the same on y-axis. The difference of x-axis is because in Figure.5.2 time axis is

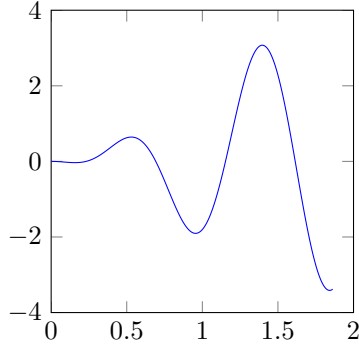


Figure 5.3: Time history of dynamic amplification factor in mid-span of the beam.
Parameters: $EJ = 2.43e10 \text{ Nm}^2$, $L = 54 \text{ m}$, $\mu = 6000 \text{ kg/m}$, $c = 29.26 \text{ m/s}$

scaled to 1 but in Figure 5.3 time is not scaled. Then it can be further concluded that Eq.5.2 and expression for ω_b are both correct.

5.5 Parameter calculation

The parameters needed for solving the explicit solution (Eq.5.2) are:

l	Length of the beam
ζ	Damping ratio
Q	Amplitude of the load
EJ	Lateral stiffness of the beam
μ	Mass per unit length
c	Speed of train

Despite parameter Q , other parameters are the fundamental attributes of bridge and vehicle which do not need further derivation. Thus this section aims to derive the expression for Q .

The expression of Q will be determined in following sequence:

Firstly a *hypothesis expression* for amplitude Q will be made depend on a *peak lateral force model*. Then the hypothesis amplitude, together with the explicit solution embedding it, will be validated by confirming if the explicit solution is able to reproduce similar results with numerical vehicle-bridge resonance simulations.¹.

Paragraphs in this section are arranged accordingly to above sequence. They are written in following layout:

¹Lateral resonance research[8, Figure.C1,C2,...,C30] provides input and output data of these simulations

1. Peak lateral model
2. Hypothesis expression for Q
3. Validation of the explicit solution

5.5.1 Peak lateral force model

The peak lateral force model is obtained by statistically fitting the peak force results of different train speeds provided by UIC research[8]. The model is expected to describe the relationship between peak lateral force and train speed.

The peak lateral force of different train types under different train speeds are presented in Table.5.1. Two figures(bold numbers) are modified² from original table. The data in the table will be used to create the speed-based expression for peak lateral force model.

Table 5.1: Peak Lateral Track Force Over All Track Qualities. Extracted From D181 Committee [8, Tab. B1]

Train type and speed	Peak lateral force(kN)		
	Locomotive	Coach/Wagon	Total
Freight 60 km/h	50	60	110
Freight 100 km/h	90	80	170
Freight 120 km/h	75	110	185
Passenger 200 km/h	140	50	190
High Speed 350 km/h	125	125	250
Passenger 200 km/h(worn)	190	80	270
High Speed 350 km/h	330	225	555

The model is created by fitting the data in Table.5.1 to a function. The function should be able to satisfy following characteristics:

1. 0kN lateral force when speed is 0km/h
2. Simply increasing in value but generally decreasing in increment³

Finally function form $F = a * v^b$ is selected because its satisfying characteristics. The first regression is conducted according to freight train data because

² The original values are 160 and 250 respectively. Output data in the table should have been filtered by standard deviation filter. The table data does not represent true maximum lateral force but a value greater than 99.5% of all force values. However, it is obvious that output data of 160kN was not filtered. It is the greatest value among all raw output data of freight train running at 100 km/h. It is not possible to calculate the explicit standard value because raw data are presented in the form of chart image. The modified value of 80kN is obtained by approximate observation. As a result, the total lateral force is modified to 170kN.

³It can be observed from Table.5.1 that the relationship between lateral force and speed is not linear. The fact that force increment decreases as speed increases can also be observed.

it possesses the most sets of data. R language was used to perform regression process.

The fitting result is presented in Formula.5.7. It is in good likelihood with original data. Achieved convergence tolerance is $2.868e - 06$. See Appendix.F for code.

$$F_{lf} = 5.2064 \cdot v^{0.7495} \quad (5.7)$$

Since 1 set of data is available for passenger train, Formula.5.7 is scaled by a constant factor to create regression for passenger trains. Please note that this regression can not be verified because lack of data. However, since freight train has a greater lateral force than passenger train, it is conservative to adopt lateral force of freight train when calculating consequences related to passenger trains. It is still reasonable to adopt this regression since passenger trains are just simply less stiff than freight trains.

The scale factor k_{pf} is obtained by comparing force value yielded by Formula.5.7 at 200km/h and original passenger train force(190kN) data at 200km/h.

$$k_{pf} = \frac{190}{a_{lf} \cdot 200^{b_{lf}}}$$

$$a_{lp} = a_{lf} \cdot k_{pf}$$

merge above two equations, yield

$$a_{lp} = \frac{190}{200^{b_{lf}}} = \frac{190}{200^{0.7495}} \approx 3.58$$

and

$$F_{lp} = a_{lp} \cdot v^{0.7495}$$

thus

$$F_{lp} = 3.58 \cdot v^{0.7495} \quad (5.8)$$

Lateral force for high speed train were obtained in same manner. The scale factor k_{hf} is obtained by comparing force value yielded by Formula.5.7 at 350km/h and original high speed train force(250kN) data at 350km/h.

$$k_{hf} = \frac{250}{a_{lf} \cdot 350^{b_{lf}}}$$

$$a_{lh} = a_{lf} \cdot k_{hf}$$

merge above two equations, yield

$$a_{lh} = \frac{250}{350^{b_{lf}}} = \frac{250}{350^{0.7495}} \approx 3.10$$

and

$$F_{lh} = a_{lh} \cdot v^{0.7495}$$

thus

$$F_{lh} = 3.10 \cdot v^{0.7495} \quad (5.9)$$

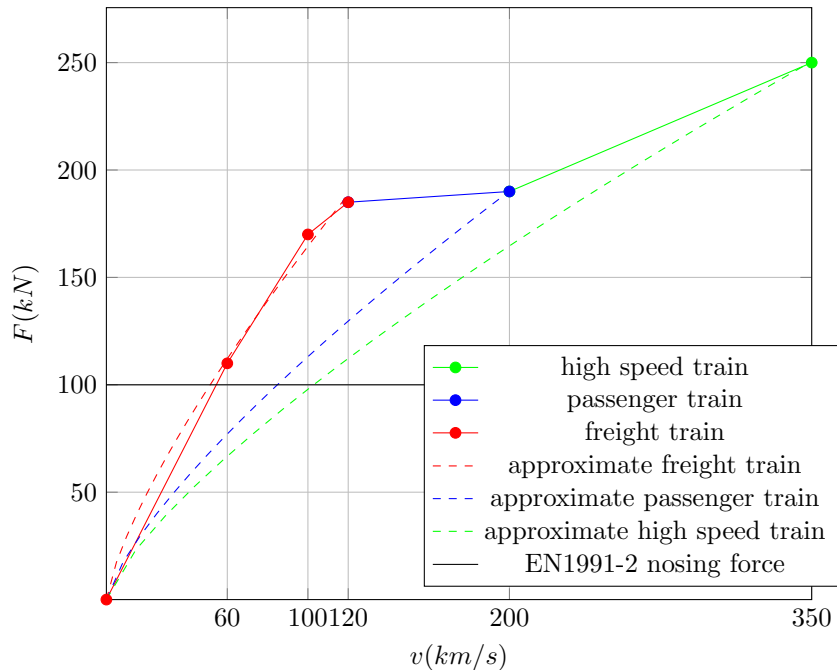


Figure 5.4: Total peak lateral track forces over all track qualities (worn profile scenario neglected)

Evaluation on the peak lateral force model By examining the magnitude of forces illustrated in Figure 5.4, it is found that these forces are not reasonable because their magnitude is obviously too high.

The reason for this phenomenon is because the force data are extracted from simulations whose track quality ranges from well-maintained to very poor⁴. Poor

⁴Up to 6mm deviation

tracks result in extremely high lateral forces, however such tracks are not allowed in the Netherlands.

The magnitude of forces can be calibrated if simulations based on realistic data of Dutch rails are provided. See Section.8.1 for recommendations on conducting simulations.

5.5.2 Hypothesis expression for amplitude Q

In this chapter a hypothesis expression for amplitude Q is obtained. The hypothesis is based on *peak lateral force model* in Section.5.5.1 and *numerical simulation results*⁵.

The numerical simulations[8, among Figure.C1,C2,...,C30] used in this section successfully produced resonance between railway vehicle and bridge. Thus they are suitable for calculating the parameters of resonance model. Simulations used in this paragraph uses input from normal tracks and wheels data which is representative for British railway tracks and vehicles in 1990s. Thus although the peak lateral force model is very conservative, the amplitude determined based on representative simulations still generates reasonable results.

There are two steps to create the hypothesis:

1. Calculate the magnitude of Q using inputs of different numerical simulation
2. Make hypothesis based on calculated magnitude

The following paragraphs of this section are written in above order.

Magnitude of Q Inputs of 3 simulation cases are selected to calculate Q . They are abbreviated to C1,C3,C9⁶ and presented in Figure.5.5,5.6 and 3.1 respectively. Q is calculated by substituting the peak displacement value of simulation output into the left hand side of the explicit solution and simulation inputs into right hand side of the same equation. With 3 sets of input and output data, 3 values of Q are obtained. They are illustrated in Table.5.2 together with the corresponding input data.

Hypothesis expression By observing calculated magnitudes of amplitude Q , it is found that Q possesses the general characteristics of peak lateral force model that the lateral force is only relevant to speed if track quality and wheel conicity are fixed. And lateral force is irrelevant to the bridge parameters.

⁵All the numerical simulation results used in this chapter are extracted from a lateral force research[8]. The correctness of these numerical simulations are verified during the research.

⁶Abbreviations are used in following paragraphs to represent simulation cases

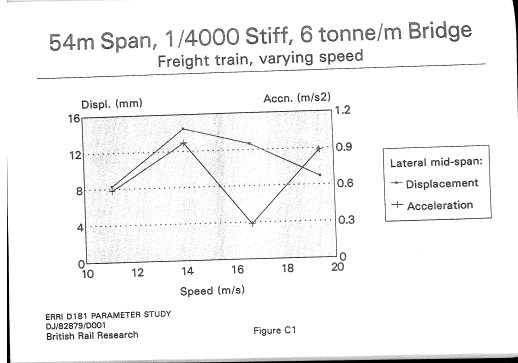


Figure 5.5: Figure C1 extracted from D181Committee [8]

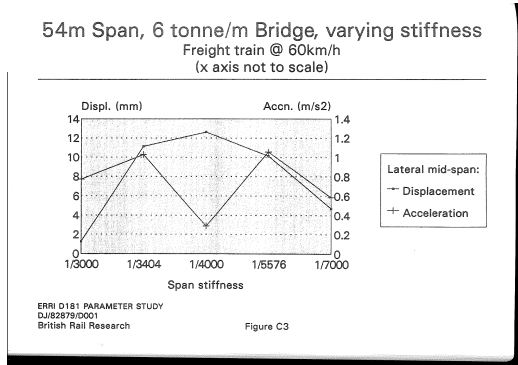


Figure 5.6: Figure C3 extracted from D181Committee [8]

Table 5.2: Parameter inputs and magnitude of amplitude Q

Parameters	Simulation cases		
	C1	C3	C9
$EJ(\delta_0/l)$	1/4000	1/4000	1/10000
$l(m)$	54m	54	120
$\mu(kg/m)$	6000	6000	6000
$c(m/s)$	14	16.67(60km/h)	14
ζ	1%	1%	1%
Train	Freight	Freight	Freight
Track	Freight	Freight	Freight
Amplitude $Q(kN)$	14	15	14

Because amplitude Q possesses the general lateral force characteristics, it is further expected that Q also has a similar form of force-speed relationship as peak lateral force model. Thus hypothesis expression is created by scaling Eq.5.7.

The exponential component does not change when scaling, so to scale the equation one set of input and output data is needed. Data ($Q = 14kN, c = 14m/s$) from C1 is selected. Please note only C1 was used in creating the hypothesis expression so C3 and C9 remains available for the verification.

The hypothesis expression for amplitude Q , which is the result of scaling, is presented in Eq.5.10.

$$Q = 1928 \times c^{0.7495} \quad (5.10)$$

Please note that this hypothesis expression is created based on a specifically chosen simulation case C1. To be scientific, expression based on other simulations will be investigated in Section.5.7.

5.6 Benchmark for the model

Since amplitude Q is a function of train speed c , the explicit solution is fully derived and only contains basic parameters. This sections aims to validate the capability of the explicit solution in yielding reasonable output.

New simulation cases⁷ C12,C13,C14⁸ are selected to take part in validation process. They are presented in Figure.5.7, 5.8 and 5.9 respectively. As mentioned above, C3 and C9 are also available for the validation, therefore there are altogether 5 sets of simulation can be used for validation.

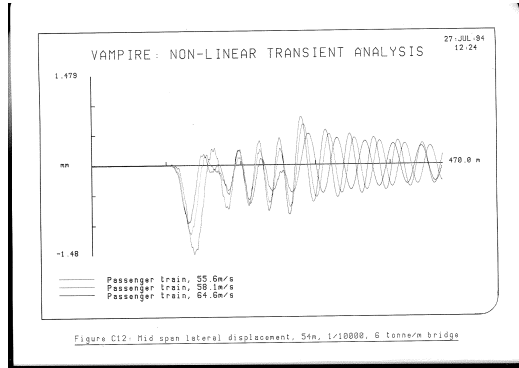


Figure 5.7: Figure C12 extracted from D181Committee [8]

⁷To assure conservativeness during the validation process, only axle repeat pattern resonance simulations are selected because their output are more pronounced than kinematic resonance effect.[8]

⁸Abbreviation in original research. These abbreviation will continually be used in the following paragraphs.

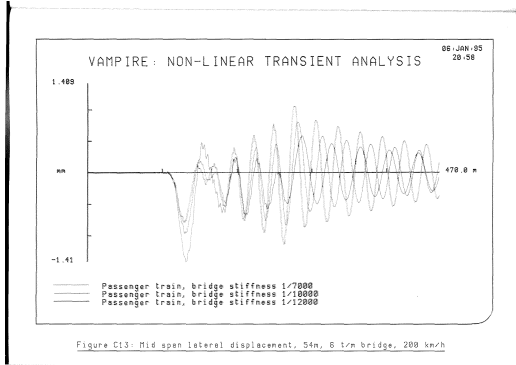


Figure 5.8: Figure C13 extracted from D181Committee [8]

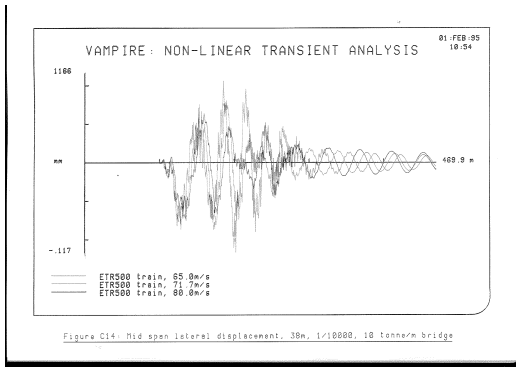


Figure 5.9: Figure C14 extracted from D181Committee [8]. An minor error is observed in y-axis label. Upper boundary of y-axis should be 0.116

The explicit solution is solved by inputting bridge parameters and trains speed of these 5 cases(C3,C9,C12,C13,C14). The results and their corresponding parameters are presented in Table.5.3.

To clearer illustrate the comparison of both peak results from simulation and explicit solution, Figure.5.10 is created with rearranged order to make descending trend more obvious.

Benchmark conclusion It can be seen that explicit solution results always keep a conservative margin above the numerical simulation results.

Difference between explicit solution and numerical simulation result for C12,C13 and C14 is bigger compared to difference for C9 and C3. It is due to the fact that the amplitude Q is calculated based on freight train lateral forces and freight trains induce greater lateral force compared to passenger trains and high speed trains(See Figure.5.4).

Table 5.3: Comparison of results of simulation output and analytical output using refined load model

Parameters	Simulation cases				
	C3	C9	C12	C13	C14
$EJ(\delta_0/t)$	1/4000	1/10000	1/10000	1/12000	1/10000
$l(m)$	54	120	54	54	38
$\mu(kg/m)$	6000	6000	6000	6000	10000
$c(m/s)$	16.67	14	55.6	55.6	65
ζ	1%	1%	1%	1%	1%
Train	Freight	Freight	Passenger	Passenger	High speed
Track	Freight	Freight	Passenger	Passenger	High speed
PSD(mm)	12.5	17.8	1.48	1.41	0.117
RES(mm)	14.1	19.7	6.6	5.8	3.0

PSD: Peak simulation displacement

RES: Result of the explicit solution

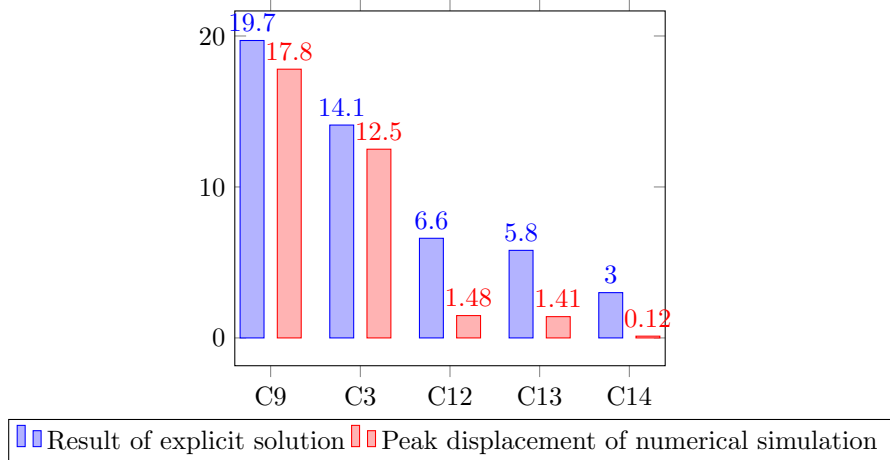


Figure 5.10: Comparison between VAMPIRE peak simulation result and analytical peak result

The descending trend of explicit solution results follows the descending trend of numerical simulation results perfectly regardless of train types.

Thus considering above reasons, the model shows satisfying performance. However, since there are few data available as benchmark, this model is still not verified for real-life application.

5.7 Supplementary parameter calculation and benchmark

Although the hypothesis expression based on C1 has been validated, this process is not generic because C1 is chosen specifically. To be scientific it is also necessary to derive expression of amplitude Q based on other 5 simulation cases.

The load equivalent amplitude of other 5 setups are calculated and their constant component are presented in the Table 5.4. Their corresponding benchmarks are presented in Table 5.5. Calculation processes are omitted because they are conducted in the same way as C1-based amplitude Q .

Table 5.4: Constant component of amplitude $Q(N)$ from all available setups

	C1	C3	C9	C12	C13	C14
	1928	1721	1760	427	463	228

Table 5.5: Benchmark of explicit solution results

Base simulation cases for Q	Analytical results of cases					
	C1	C3	C9	C12	C13	C14
C1	0.0145	0.0141	0.0197	0.0066	0.0058	0.003
C3	0.013	0.0125	0.0174	0.0059	0.0051	0.0036
C9	0.013	0.0128	0.0178	0.0061	0.0053	0.0032
C12	0.0032	0.0031	0.0043	0.00148	0.0013	0.0008
C13	0.0035	0.0034	0.0047	0.0016	0.00141	0.0002
C14	0.0021	0.0020	0.0028	0.0010	0.0008	0.00012
Simulation Peak Displacement	0.014	0.0125	0.0178	0.00148	0.00141	0.00012

Among all amplitude Q , the one created from C1 is most satisfying because its outputs are all conservative towards numerical simulation output. Other amplitude shows at least one nonconservative output.

It can also be observed that the results of C12, C13 and C14 are unacceptable due to the reason that their output are too small compared to numerical simulation output. They can't predict reliable result for C1, C3 and C9.

Since there is few data available, it's meaningless to conduct further statistical procedures. The rest of the thesis will use amplitude Q base C1 because it is conservative on all benchmark.

5.8 Evaluation on the model

A simplified model for checking lateral resonance response of railway bridge is developed in this chapter. This model is capable of simulating a resonance scenario where the bridge is passed by a moving railway vehicle. However, several disadvantages of the current model should be noted:

1. Only one concentrated force is modeled to represent the lateral dynamic effect induced by railway vehicle. It means the load in the model can not represent the distribution of vehicle axle forces.
2. Amplitude Q is calculated based on a specifically chosen numerical simulation case. However, the aim of the model is to generically simulate vehicle-bridge response behavior, and such specifically choosing may be against this principle of generic.
3. The model is not fully validated because of the small quantity of available simulation results for validation. These simulation scenarios can not represent generic real-life scenarios.
4. The model is not calibrated for modern Dutch railway because model parameter Q is based on data generated by old railway vehicles.⁹

⁹Simulations[8] were conducted during 1990s using parameters extracted from real trains at the time. Compared to trains of 1990s, modern railway vehicles possess more sophisticated suspension systems designed to suppress the lateral motion of the vehicle thus they are expected to induce lower lateral forces to tracks.

Chapter 6

Practical usage of simplified model

In practical usage, the speed that generates the highest peak response is unknown. Thus it is necessary to obtain the peak response for all speeds within the possible speed range. This is done by iteratively solving the explicit solution Eq.5.2 with a speed range. The increment in speed iteration is set in a way that ensures at least 1000 runs are done to guarantee precession. An example is illustrated as follows to show the usage on a real bridge project.

A case study is done to illustrate the work flow in using the simplified model. Matlab scripts are written to automate the process. Scripts are presented in Appendix.G.

6.1 Case study

For an arch railway bridge located near Amsterdam, first step to is to collect following parameters:

$$L = 255m, m = 5222e3kg, \mu = 2.0478e4kg/m, EJ = 6.56e12Nm^2$$

where:

L : span of the bridge

μ : uniform mass per unit length of the bridge

EJ : lateral stiffness of the bridge

to test through a speed range of $1m/s - 30m/s$

By inputting following command into Matlab console¹,

```
>>Speedenvelop(6.56e12,255,2.0478e4,1,30,0.01)
```

the envelop for displacement is generated and illustrated in Figure.6.1

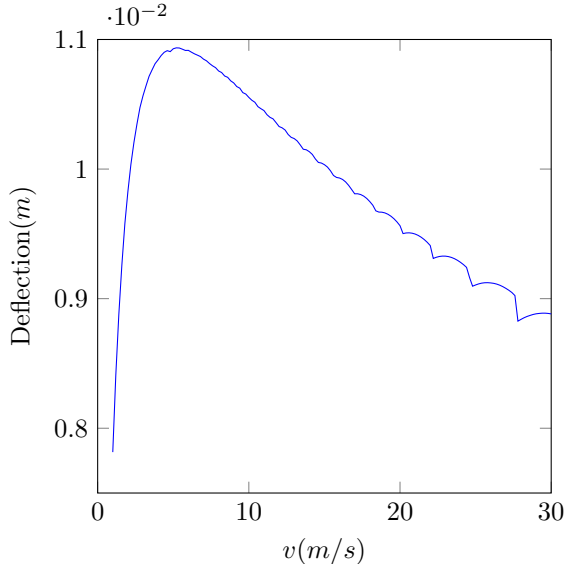


Figure 6.1: Peak deflection at mid-span with regard to changing train speed. Parameters: $EJ = 6.56e12 \text{Nm}^2$, $L = 255\text{m}$, $\mu = 20478\text{kg/m}$, $c_{min} = 1\text{m/s}$, $c_{max} = 30\text{m/s}$

The plot shows that the critical speed appears at approximately 5m/s and corresponding peak deflection response is approximately 11mm.

Since the relationship between end support rotation angle and mid-span deflection is widely known as:

$$\varphi = \frac{3}{L} \cdot \delta_0$$

and rotation is yielded as:

$$\varphi = \frac{3}{255} \times 0.011 = 0.00013$$

This value is much lower than the rotation value regulated in EN1991-2. See Section.A.3.3.1 for criteria details.

Thus the conclusion can be made that this bridge is safe subjected to lateral dynamic load.

¹Before beginning the calculation, make sure fog.m and Speedenvelop.m are in current working directory.

6.2 Conclusion

A general conclusion of practical method is, for a certain bridge, faster train speed does not necessary result in higher resonance response of the bridge. As can be seen in Figure.6.1, critical speed appears at approximately $5m/s$, and response start to fall when speed is higher than $5m/s$. This means comparing to higher load amplitude caused by higher train speed, the shorter loading time caused by same reason is more dominating. By considering the fact in Figure.5.10 that the explicit solution is even more conservative for higher speed. It can be concluded that high-speed trains cause less dynamic problem for lateral bridge dynamics.

Matlab scripts are already written and attached for the convenience of designers. Since the explicit solution has been given in the chapter, it's completely possible to adopt them in other mathematical software for different preferences.

Chapter 7

Conclusion

This thesis successfully fulfilled the required tasks in the research objectives and question.

To assist the design of a long-span bridge of Iv-infra, a simplified model for assessing lateral bridge resonance behavior is developed in this thesis. This model is validated to be conservative and reasonable by benchmark.

However, due to the lack of data available in creating the model, the model is not validated to be applied universally on real-life project. Currently it has following disadvantages:

1. Only one concentrated force is modeled to represent the lateral dynamic effect induced by railway vehicle. It means the load in the model can not represent the distribution of vehicle axle forces.
2. Amplitude Q is calculated based on a specifically chosen numerical simulation case. However, the aim of the model is to generically simulate vehicle-bridge response behavior, and such specifically choosing may be against this principle of generic.
3. The model is not fully validated because of the small quantity of available simulation results for validation. These simulation scenarios can not represent generic real-life scenarios.
4. The model is not calibrated for modern Dutch railway because model parameter Q is based on data generated by old railway vehicles.¹
5. The longest bridge in numerical simulation is 120m long. Thus the model is not validated for bridges longer than 120m.

¹Simulations[8] were conducted during 1990s using parameters extracted from real trains at the time. Compared to trains of 1990s, modern railway vehicles possess more sophisticated suspension systems designed to suppress the lateral motion of the vehicle thus they are expected to induce lower lateral forces to tracks.

Despite the disadvantages of the current model, it provides a direction of analyzing lateral dynamics of railway bridges which is different from nowadays available analyzing techniques. It offers a simple approach to avoid heavy numerical simulations during the analysis and therefore, saves the effort and cost for designers. The model shall be regarded as a prototype that can be improved and expanded by future researches. See Chapter.8 for details of recommendations for future researches.

Chapter 8

Recommendations for future researches

The recommendations aims to guide future researches to be conducted according to the disadvantages mentioned in previous chapter.

General recommendations:

1. Improve the model by make more sophisticated assumption to better reflect real-life scenario. For example: use more than one concentrated force to represent the lateral dynamic load.
2. It is recommended to use a larger database when determining the expression for parameters.
3. Conduct more numerical simulations to provide database for the sake of creation and validation of the model. See Section 8.1 for detailed explanation on how to conduct these simulations.

8.1 Recommendations on numerical simulations

More accurate statistical result can be yielded with more simulation data. Since now only 6 sets of data are used, the simplified model is not globally reliable. However, it is recommended that future research uses a larger simulation data base to further improve the accuracy of the model.

It is possible to modify the amplitude of the model to a less conservative value according to newly conducted simulations. It is expected that newly conducted simulations yield smaller lateral force on tracks because of the advanced suspension systems implemented in modern vehicle designs and better track quality.

Therefore, numerical simulations are recommended to be conducted according to following suggestions:

1. Use more realistic and up-to-date data on modern Dutch train vehicles and railway. The result will help the model to be applicable for Dutch bridges.
2. Investigate over a broader range of bridge span(greater than 150m).

Appendices

Appendix A

Literature Review of regulations regarding lateral railway bridge dynamics in 1991-2

Eurocode 1990 and Eurocode 1991-2 and their corresponding National Annex are primary codes to be fulfilled through out the whole process of conducting a railway bridge in Netherlands. It is of great importance to study dynamic effect on railway bridges due to increasing usage of public train service.

This literature review aims to filter out criteria and requirements related to lateral railway bridge dynamics in EN1991-2.

A.1 Factors influencing dynamic behaviour

As stated inCEN [4, 6.4.2] there are 11 factors influencing dynamic behaviour of a railway bridge. The principal factors which influence dynamic behaviour are:

- the speed of traffic across the bridge
- the span L of the element and the influence line length for deflection of the element being considered
- the mass of the structure
- the natural frequencies of the whole structure and relevant elements of the structure and the associated mode shapes (eigenforms) along the line of

the track

- the number of axles, axle loads and the spacing of axles
- the damping of the structure
- vertical irregularities in the track
- the unsprung/sprung mass and suspension characteristics of the vehicle
- the presence of regularly spaced supports of the deck slab and/or track (cross girders, sleepers etc.)
- vehicle imperfections (wheel flats, out of round wheels, suspension defects etc.)
- the dynamic characteristics of the track (ballast, sleepers, track components etc.)

Other factors may include:

1. The track number of the bridge and their alignment.
2. Multiple trains running on bridge simultaneously.
3. Track alignment

A.2 Requirements for railway bridge verification

CEN [5] propose following requirements. Criteria regarding lateral direction are bolded.

1. Checks on bridge deformations shall be performed for traffic safety purposes for the following items:
 - vertical accelerations of the deck
 - vertical deflection of the deck throughout each span
 - unrestrained uplift at the bearings(to avoid premature bearing failure)
 - vertical deflection of the end of the deck beyond bearings(to avoid destabilising the track, limit uplift forces on rail fastening systems and limit additional rail stresses)
 - twist of the deck measured along the centre line of each track on the approaches to a bridge and across a bridge(to minimise the risk of train derailment)

- rotation of the ends of each deck about a transverse axis or the relative total rotation between adjacent deck ends(to limit additional rail stresses, limit uplift forces on rail fastening systems and limit angular discontinuity at expansion devices and switch blades)
 - longitudinal displacement of the end of the upper surface of the deck due to longitudinal displacement and rotation of the deck end(to limit additional rail stresses and minimise disturbance to track ballast and adjacent track formation)
 - **horizontal transverse deflection(to ensure acceptable horizontal track radii)**
 - **horizontal rotation of a deck about a vertical axis at ends of a deck (to ensure acceptable horizontal track geometry and passenger comfort)**
 - **limits on the first natural frequency of lateral vibration of the span to avoid the occurrence of resonance between the lateral motion of vehicles on their suspension and the bridge**
2. Checks on bridge deformations should be performed for passenger comfort, i.e. vertical deflection of the deck to limit coach body acceleration in accordance with A2.4.4.3CEN [5]
 3. The limits given in A2.4.4.2 and A2.4.4.3CEN [5] take into account the mitigating effects of track maintenance (for example to overcome the effects of the settlement of foundations, creep, etc.)

A.3 Horizontal transverse dynamic effects

There's only one criterion in the Eurocodes mentiones that the bridge's first lateral natural frequency should not be lower than 1.2 Hz.

However, as more and more long-span bridges are built nowadays, this requirement is not valid for more bridges. This is because, in general, the lateral natural frequency of a bridge decreases when span increases. For bridges with span longer than 150m, there's few bridge can have a lateral frequency higher than 1.2Hz, according to senior engineers' designing experience.

So it is vital to discuss horizontal dynamic effects for the sake of longer span bridges. In addition, a study has been carried out on the requirements for horizontal vibration of railway bridges to make the results of dynamic analysis usable.

A.3.1 Nosing force

Nosing force is defined in Eurocode 1991-2. Its original background can be found in D181Committee [7, Proposed criteria]. It is defined as a representation of actions, in combine with actions like vertical loads, dynamic effects, centrifugal forces, traction and braking forces, etc.

The evidence of RP6 is the background of nosing force in EN1991-2 is the following repeating literature:

In CEN [4, 6.5.2]:

(1)P The nosing force shall be taken as a concentrated force acting horizontally, at the top of the rails, perpendicular to the centre-line of track. It shall be applied on both straight track....

In D181Committee [7, 4.1B]:

These forces shall be applied at the top of the rails in the most unfavourable position and acting horizontally, perpendicular to the track centreline...

With another statement also helps proofing RP6 is the background of nosing force in EN1991-2 in D181Committee [7, 4:Draft Recommendations]:

These can therefore be expressed as follows: (Article **6.5.2** of ENV 1991-3 of 1994)...

ENV 1991-3 was renamed to EN 1991-2 in 2003.

Originally in D181Committee [7, 4:Draft Recommendations], nosing forces was defined as lateral forces from vehicle/bridge interaction as a result of **hunting**.

The characteristic value of the nosing force shall be taken as $Q_{sk} = 100kN$. It shall not be multiplied by the factor Φ (CEN [4, 6.45]) or by the factor f in CEN [4, 6.51].

The characteristic value of the nosing force should be multiplied by the factor α in accordance with CEN [4, 6.3.2] for values of $\alpha \geq 1$

The nosing force shall always be combined with a vertical traffic load.

A.3.2 Verification of the Limit States

CEN [4, 6.4.6.5] proposes following principles to be followed during design:

To ensure traffic safety:

1. The verification of maximum peak deck acceleration shall be regarded as a traffic safety requirement checked at the serviceability limit state for the prevention of track instability

2. The dynamic enhancement of load effects shall be allowed for by multiplying the static loading by the dynamic factor Φ defined in CEN [4, 6.4.5]. If a dynamic analysis is necessary, the results of the dynamic analysis shall be compared with the results of the static analysis enhanced by Φ (and if required multiplied by α in accordance with CEN [4, 6.3.2]) and the most unfavourable load effects shall be used for the bridge design.
3. If a dynamic analysis is necessary, a check shall be carried out according to CEN [4, 6.4.6.6] to establish whether the additional fatigue loading at high speeds and at resonance is covered by consideration of the stresses due to load effects from $\Phi \times LM71$ (and if required $\Phi \times LoadModelSW/0$ for continuous structures and classified vertical load in accordance with CEN [4, 6.3.2(3)] where required). The most adverse fatigue loading shall be used in the design.

A.3.3 Serviceability limit states - traffic safety

A.3.3.1 Transverse deformations and vibrations

199 [1, A2.4.4.2.4] proposed that transverse deformation and vibration of the deck shall be checked for characteristic combinations of Load Model 71 and SW/0 as appropriate multiplied by the dynamic factor ϕ and α (or real train with the relevant dynamic factor if appropriate), wind loads, nosing force, centrifugal forces in accordance with CEN [4, 6] and the effect of a transverse temperature differential across the bridge.

The transverse deflection δ_h at the top of the deck should be limited to ensure:

1. a horizontal angle of rotation of the end of a deck about a vertical axis not greater than the values given in Table. A.1 , or
2. the change of radius of the track across a deck is not greater than the values in Table. A.1 , or
3. at the end of a deck the differential transverse deflection between the deck and adjacent track formation or between adjacent decks does not exceed the specified value

The first natural frequency of lateral vibration of a span should not be less than f_{h0} . The value for f_{h0} may be defined in the National Annex. The recommended value is: $f_{h0} = 1.2\text{Hz}$

Evidence of D181Committee [7] is the origin of CEN [4, A.2.4.4.2.4(3)] is found in D181Committee [7, p4.2: Lateral Frequencies]:

In order to avoid the phenomena of lateral resonance in vehicles, the first natural frequency of lateral vibration of the span f_{lt} such that:

Speed range V(km/h)	Maximum horizontal rotation(radian)	Maximum change of radius of curvature
	Single deck	Multi-deck bridge
$V \leq 120$	α_1	r_1
$120 \leq V \leq 200$	α_2	r_2
$V > 200$	α_3	r_3
		r_4
		r_5
		r_6

NOTE 1 The change of the radius of curvature may be determined using:

$$r = \frac{L^2}{8\delta_h}$$

NOTE 2 The transverse deformation includes the deformation of the bridge deck and the substructure(including piers, piles and foundations).

NOTE 3 The values for the set of α_i and r_i may be defined in the National Annex. The recommended values are:

$$\begin{aligned} \alpha_1 &= 0.0035; \alpha_2 = 0.0020; \alpha_3 = 0.0015; \\ r_1 &= 1700; r_2 = 6000; r_3 = 14000; \\ r_4 &= 3500; r_5 = 9500; r_6 = 17500 \end{aligned}$$

Table A.1: Maximum horizontal rotation and maximum change of radius of curvature

$$f_{lt} \geq 1.2 \text{Hz}$$

Until now there's no further instructions in EN1991-2 for bridges which can not pass 1.2Hz criterion. However, for bridges longer than 100 meters, they are almost guaranteed to fail 1.2Hz criterion.

A.4 Conclusion

By reviewing EN1991-2 thoroughly, it is found that there are altogether two regulations regarding lateral dynamics of railway bridges. They are:

1. Nosing force(action)
2. 1.2Hz criterion

Although vertical dynamics of railway bridges is focused a lot, there's only two statements about lateral dynamics of railway bridges. What's more, there's no quantifying criteria even if a dynamic analysis is done.

These two regulations have the same background documents: D181 report series.
The analysis of D181 report series will be carried out in following chapter.

Appendix B

General information of report series D181 and its selected documents

B.1 Structure of report series

Reports involved in the series are listed below in the order of publishing time:

1. RP 1: Summaries of national standards and literature survey
2. RP 2: Submitted programs and example of application
3. RP 3: Dynamic measurements on the steel bridge over the Brenta river on the MilanVenice line at 234 + 0.963 km
4. RP 4: Dynamic measurements on steel bridges over the Vh river by Sala on the MarcheggSzob line at 117 748 km
5. DT 312: Etude de l'influence de la frquence du filtre sur les valeurs mesures des forces verticales et latrales sur les rails
6. RP 5: Dynamic measurements on the metal arched bridge on PKP
7. DT 313: Analyse des dformations latrales d'un pont souple (cas du PONT de LIXHE) Ligne SNCB de TONGRESMONTZEN par J.J. REBER SBB Bau GD
8. DT 329: Parametric study Part 1: Parametric study Initial phase (September 1994) Part 2: Parametric study Phase 2 (February 1995) Authors: L.T. James and G.A. Scott
9. RP 6: Final Report

In this thesis document DT 329 and document RP 6 are obtained and studied, but other reports in English version are not available to the researcher.

B.2 Modelling of Parametric Research DT329

A special version of VAMPIRE with bridge module implemented was used to run simulation analysis.

For an overview of modelling setup in both research phases, see Figure B.1. Following paragraphs will give details of modelling.

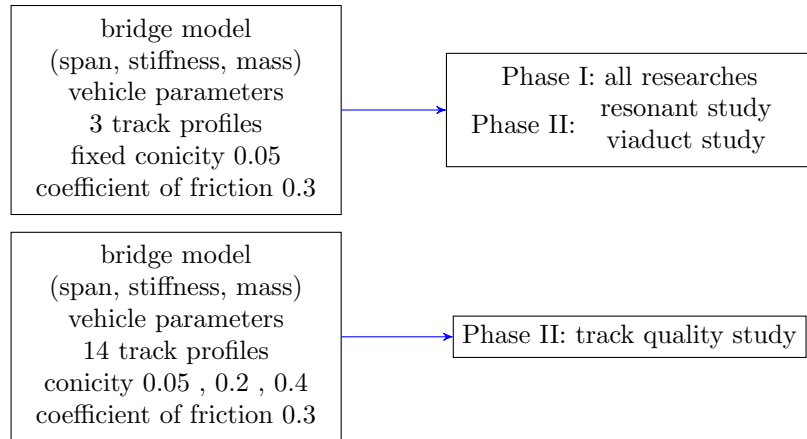


Figure B.1: Overview of modelling setups for different studies conducted in DT329

B.2.1 Model of bridge

The bridge cases were modelled by assuming the bridges to behave as simply supported uniform beams. Transverse beam theory was then used to determine the frequencies and mode shapes of vibration for a given combination of span, mass per unit length and flexural rigidity. The modal information for the bridge was then used in a 'Normal Modes' analysis of the bridge.

For each case, all lateral modes of vibration up to and including 20 Hz were used. In order to prevent this artificially over-simplifying the model, if fewer than five modes were 20 Hz or less, all of the first five were used.

B.2.2 Bridge parameters

The spans considered were: 20 m, 33 m, 54 m, 90 m and 120 m. The flexibilities, defined as deflection of mid span over span length due to a static point load of

100 kN at mid span, are: 1/4000, 1/10000, and 1/20000. The mass per unit lengths required are: 2 tonnes/m, 6 tonnes/m, and 10 tonnes/m.

For the initial phase, see Figure B.2 for a selection of eleven of the possible combinations examined.

Span	Flexibility	Mass/Length	Cases
20	1/10000	6	36-40, 52
33	1/10000	6	41-43
54	1/4000	2	16-20
54	1/4000	10	21-25
54	1/10000	2	1-5
54	1/10000	6	6-10
54	1/10000	10	11-15
54	1/20000	2	26-30
54	1/20000	10	31-35
90	1/10000	6	44-46
120	1/10000	6	47-51

Figure B.2: Bridge parameter combination

B.2.3 Vehicle parameters

Three train types are considered: a typical freight train, a typical standard passenger train, and a typical high speed passenger train. Appendix.C details the parameters used to construct each model. In general, each model consists of a locomotive and a number of identical vehicles appropriate to the train type. The total number of axles in each train is 24. Although effects on the train are only examined on the first vehicle of each type, extra vehicles are added to the train to see what cumulative effects occur to the bridge.

The freight train consists of a British Railways Class 56 locomotive and nine UIC wagons. This has a total length of 131.56 m, which assumes a nominal vehicle coupling distance of 4 m. Runs at 60 km/h and 100 km/h are required.

The standard passenger train consists of an E444 locomotive and five UIC coaches. This has a total length of 143.8 m. It is based on one of two train

models used as part of the study of the FS Bridge discussed in report RP 3 of the Committee, differing only by the addition of three extra coaches. This is required to run at 160 km/h and 200 km/h.

The high speed passenger train consists of an ETR500 locomotive and five ETR500 coaches, having a total length of 145.8 m. It is based on the other FS bridge study train model mentioned above, differing from the original by an additional three ETR500 coaches. It is required to run at 300 km/h and 350 km/h.

B.2.4 Track

For initial study phase, the track samples used were consistent with each train type. PSD plots of each are shown in Figures C.13 to C.15. Sample TRACK-FRT.DAT was used for all analysis runs for the freight train. This is measured data from a typical BR freight line. Sample TRACKPKN.DAT was used for the standard passenger train analysis runs. This is measured data from a part of the BR East Coast main line. Sample TRACKPH.DAT was used for high speed passenger train analysis runs. This is measured data from a typical DB high speed line.

Samples of 500 m were chosen so that there would be 100 m before the bridge and at least 100 m after the bridge for all combinations of span and train length. The initial 100 m is required to check vehicle behaviour on the track irregularity alone, and the portion after the train has left the bridge is required to check that the bridge vibrations decay.

For secondary study phase, the track data used to excite the mathematical models was taken from the British Rail Research library of measured track data. For the viaduct and resonance investigations, the track files used were the same as those used in the first part of the study. For the investigation of the influence of track quality, additional track data was used so as to give the widest possible range of realistic track qualities.

B.2.5 Contact data

For each run the same contact data was used, consisting of rails inclined at 1:20, and wheel profiles of conicity of 0.05 (based on standard British Rail 113A rails and PI wheel profiles). The coefficient of friction applied was 0.3.

B.2.6 Data produced

For every analysis run the following results were obtained at intervals of 0.01 seconds.

BRIDGE DATA:

Lateral displacement at mid span Lateral acceleration at mid span

VEHICLE LATERAL ACCELERATION DATA:

Loco body at leading pivot

Leading coach/wagon body at leading pivot/axle

Loco leading bogie

Leading coach/wagon leading bogie/axle

TOTAL LATERAL FORCE DATA:

Loco leading bogie

Leading coach/wagon leading bogie/axle

LATERAL FORCES ON INDIVIDUAL WHEELS

Leading coach/wagon, first axle, left and right wheels

Leading coach/wagon, second axle, left and right wheels

Loco, first axle, left and right wheels

Loco, second axle, left and right wheels

In addition, for freight train runs, since the locomotive has two bogies of three axles, the forces on the individual wheels of the third axle were also produced.

Peak values for each of the outputs produced for the required ranges were obtained. For bridge outputs, peak values were taken for the period where any part of the train was on the bridge. For loco and leading coach/wagon outputs, peak values were taken whilst the vehicle in question was in contact with the bridge.

Peak values for each output were then read into a spread sheet where they could be compared more easily to check for emerging trends. The spread sheet has been partially automated to produce graphs of a single output for each train type for a single varying bridge parameter, for given values of the other bridge parameters. Figures 4 to 30 of original D181Committee [8] report show typical plots which have been produced in this manner.

Appendix C

Plots and diagrams used in D181 DT 329

Freight train: Principle axle repeat patterns	dist m	Speed	
		60 km/h	100 km/h
wagon n axle 2 - wagon n+1 axle 1	4.00	4.17	6.94
wagon wheelbase	9.00	1.85	3.09
wagon n axle m - wagon n+1 axle m	13.0	1.28	2.14
wagon n axle m - wagon n+2 axle m	26.0	0.64	1.07
Passenger train: Principle axle repeat patterns	dist m	Speed	
		160 km/h	200 km/h
coach n axle 1 - 2, and coach n axle 3 - 4	2.56	17.36	21.70
coach n axle m - coach n+1 axle m	26.4	1.68	2.10
coach n axle m - coach n+2 axle m	52.8	0.84	1.05
ETR 500 train: Principle axle repeat patterns	dist m	Speed	
		300 km/h	350 km/h
coach n axle 1 - 2 and coach n axle 3 - 4	3.0	27.78	32.41
coach n axle m - coach n+1 axle m	26.1	3.19	3.72
coach n axle m - coach n+2 axle m	52.2	1.60	1.86
coach n axle m - coach n+3 axle m	69.3	1.20	1.40

Table C.1: Axle repeat patterns and typical frequencies. Extracted from D181 Committee [8, Appendix C]

Kinematic wavelength, m	Freight train	Passenger train	ETR500 train
Locomotive	39 - 45	32 - 38	39 - 45
Coach/wagon	24 - 39	34 - 38	36 - 40

Table C.2: Kinematic wavelength ranges per vehicle, with BR P1 profiles. Extracted from D181Committee [8, Appendix C]

VEHICLE MODEL PARAMETER LISTS**VEHICLE TITLE BR CLASS 56 LOCOMOTIVE****MASSES & INERTIAS**

Number of bogies	2
Number of axles (per bogie)	3
Body mass	81.2 Mg
Body roll inertia	107.0 Mgm ²
Body pitch inertia	1400.0 Mgm ²
Body yaw inertia	1400.0 Mgm ²
Bogie mass	5.6 Mg
Bogie roll inertia	5.0 Mgm ²
Bogie pitch inertia	21.6 Mgm ²
Bogie yaw inertia	21.6 Mgm ²
Wheelset mass	2.2 Mg
Wheelset roll and yaw inertia	2.7 Mgm ²

DIMENSIONS

Semi pivot spacing	5.19 m
Semi wheelbase	2.09 m
Wheel radius	0.57 m
Body centre of gravity height above rail level	1.85 m
Bogie centre of gravity height above rail level	0.86 m

PRIMARY SUSPENSION

Lateral stiffness (per axle)	0.1 MN/m
Vertical stiffness (per axle)	2.63 MN/m
Yaw stiffness (per axle)	29.0 MNm/r
Lateral damper rate (per axle)	- MNs/m
Vertical damper rate (per axle)	0.05 MNs/m
Vertical friction breakout (per axle)	- KN
Height above rail level of lateral springs	0.67 m
Lateral semi spacing of vertical springs	1.035 m
Height above rail level of lateral dampers	- m
Lateral semi spacing of vertical dampers	1.035 m
Lateral semi spacing of vertical friction	- m

Figure C.1: BR CLASS 56 LOCOMOTIVE. Extract from D181Committee [8, Appendix 2]

Appendix 2

SECONDARY SUSPENSION

Lateral stiffness (per bogie)	0.77 MN/m
Vertical stiffness (per bogie)	2.72 MN/m
Roll bar stiffness (per bogie)	- MNm/r
Yaw stiffness (per bogie)	1.22 MNm/r
Lateral damper rate (per bogie)	0.084 MNs/m
Vertical damper rate (per bogie)	0.15 MNs/m
Yaw damper rate (per bogie)	0.055 MNms/r
Height above rail level of lateral springs	1.31 m
Lateral semi spacing of vertical springs	1.062 m
Height above rail level of lateral dampers	1.06 m
Lateral semi spacing of vertical dampers	1.062 m

Figure C.2: BR CLASS 56 LOCOMOTIVE. Extract from D181Committee [8, Appendix 2]

Appendix 2

VEHICLE TITLE UIC FREIGHT WAGON (LADEN)

MASSES & INERTIAS

Number of bogies	-
Number of axles (per wagon)	2
Body mass	41.0 Mg
Body roll inertia	35.0 Mgm ²
Body pitch inertia	500.0 Mgm ²
Body yaw inertia	500.0 Mgm ²
Bogie mass	- Mg
Bogie roll inertia	- Mgm ²
Bogie pitch inertia	- Mgm ²
Bogie yaw inertia	- Mgm ²
Wheelset mass	2.0 Mg
Wheelset roll and yaw inertia	1.7 Mgm ²

DIMENSIONS

Semi pivot spacing	- m
Semi wheelbase	4.5 m
Wheel radius	0.46 m
Body centre of gravity height above rail level	1.5 m
Bogie centre of gravity height above rail level	- m

PRIMARY SUSPENSION

Lateral stiffness (per axle)	1.5 MN/m
Vertical stiffness (per axle)	2.6 MN/m
Yaw stiffness (per axle)	10.0 MNm/r
Lateral damper rate (per axle)	0.034 MNs/m
Vertical damper rate (per axle)	- MNs/m
Vertical friction breakout (per axle)	3.0 KN
Height above rail level of lateral springs	0.46 m
Lateral semi spacing of vertical springs	1.0 m
Height above rail level of lateral dampers	0.46 m
Lateral semi spacing of vertical dampers	- m
Lateral semi spacing of vertical friction	1.0 m

958223/01

3

Figure C.3: UIC FREIGHT WAGON (LADEN). Extract from D181Committee [8, Appendix 2]

Appendix 2

SECONDARY SUSPENSION

Lateral stiffness (per bogie)	- MN/m
Vertical stiffness (per bogie)	- MN/m
Roll bar stiffness (per bogie)	- MNm/r
Yaw stiffness (per bogie)	- MNm/r
Lateral damper rate (per bogie)	- MNs/m
Vertical damper rate (per bogie)	- MNs/m
Yaw damper rate (per bogie)	- MNms/r
Height above rail level of lateral springs	- m
Lateral semi spacing of vertical springs	- m
Height above rail level of lateral dampers	- m
Lateral semi spacing of vertical dampers	- m

Figure C.4: UIC FREIGHT WAGON (LADEN). Extract from D181Committee [8, Appendix 2]

Appendix 2

VEHICLE TITLE FS ETR500 LOCOMOTIVE

MASSES & INERTIAS

Number of bogies	2
Number of axles (per bogie)	2
Body mass	55.98 Mg
Body roll inertia	53.366 Mgm ²
Body pitch inertia	1643.0 Mgm ²
Body yaw inertia	1630.0 Mgm ²
Bogie mass	3.896 Mg
Bogie roll inertia	3.115 Mgm ²
Bogie pitch inertia	5.843 Mgm ²
Bogie yaw inertia	8.107 Mgm ²
Wheelset mass	2.059 Mg
Wheelset roll and yaw inertia	1.164 Mgm ²

DIMENSIONS

Semi pivot spacing	6.0 m
Semi wheelbase	1.5 m
Wheel radius	0.55 m
Body centre of gravity height above rail level	1.65 m
Bogie centre of gravity height above rail level	0.64 m

PRIMARY SUSPENSION

Lateral stiffness (per axle)	12.0 MN/m
Vertical stiffness (per axle)	3.55 MN/m
Yaw stiffness (per axle)	15.4 MNm/r
Lateral damper rate (per axle)	- MNs/m
Vertical damper rate (per axle)	0.3 MNs/m
Vertical friction breakout (per axle)	- KN
Height above rail level of lateral springs	0.55 m
Lateral semi spacing of vertical springs	1.03 m
Height above rail level of lateral dampers	- m
Lateral semi spacing of vertical dampers	1.2 m
Lateral semi spacing of vertical friction	- m

958223/01

5

Figure C.5: FS ETR500 LOCOMOTIVE. Extract from D181 Committee [8, Appendix 2]

Appendix 2

SECONDARY SUSPENSION

Lateral stiffness (per bogie)	0.584 MN/m
Vertical stiffness (per bogie)	1.888 MN/m
Roll bar stiffness (per bogie)	1.0 MNm/r
Yaw stiffness (per bogie)	- MNm/r
Lateral damper rate (per bogie)	0.037 MNs/m
Vertical damper rate (per bogie)	0.145 MNs/m
Yaw damper rate (per bogie)	0.938 MNms/r
Height above rail level of lateral springs	0.95 m
Lateral semi spacing of vertical springs	1.03 m
Height above rail level of lateral dampers	0.73 m
Lateral semi spacing of vertical dampers	1.05 m

Figure C.6: FS ETR500 LOCOMOTIVE. Extract from D181 Committee [8, Appendix 2]

Appendix 2

VEHICLE TITLE FS ETR500 COACH

MASSES & INERTIAS

Number of bogies	2
Number of axles (per bogie)	2
Body mass	34.23 Mg
Body roll inertia	54.63 Mgm ²
Body pitch inertia	1821.0 Mgm ²
Body yaw inertia	1760.0 Mgm ²
Bogie mass	2.76 Mg
Bogie roll inertia	2.034 Mgm ²
Bogie pitch inertia	2.504 Mgm ²
Bogie yaw inertia	4.071 Mgm ²
Wheelset mass	1.58 Mg
Wheelset roll and yaw inertia	0.753 Mgm ²

DIMENSIONS

Semi pivot spacing	9.5 m
Semi wheelbase	1.5 m
Wheel radius	0.44 m
Body centre of gravity height above rail level	1.5 m
Bogie centre of gravity height above rail level	0.68 m

PRIMARY SUSPENSION

Lateral stiffness (per axle)	4.35 MN/m
Vertical stiffness (per axle)	1.61 MN/m
Yaw stiffness (per axle)	14.0 MNm/r
Lateral damper rate (per axle)	- MNs/m
Vertical damper rate (per axle)	0.015 MNs/m
Vertical friction breakout (per axle)	- KN
Height above rail level of lateral springs	0.44 m
Lateral semi spacing of vertical springs	0.96 m
Height above rail level of lateral dampers	- m
Lateral semi spacing of vertical dampers	0.96 m
Lateral semi spacing of vertical friction	- m

958223/01

7

Figure C.7: FS ETR500 COACH. Extract from D181Committee [8, Appendix 2]

Appendix 2

SECONDARY SUSPENSION

Lateral stiffness (per bogie)	0.256 MN/m
Vertical stiffness (per bogie)	0.722 MN/m
Roll bar stiffness (per bogie)	1.0 MNm/r
Yaw stiffness (per bogie)	- MNm/r
Lateral damper rate (per bogie)	0.04 MNs/m
Vertical damper rate (per bogie)	0.065 MNs/m
Yaw damper rate (per bogie)	0.70 MNms/r
Height above rail level of lateral springs	0.8 m
Lateral semi spacing of vertical springs	0.96 m
Height above rail level of lateral dampers	0.8 m
Lateral semi spacing of vertical dampers	1.2 m

Figure C.8: FS ETR500 COACH. Extract from D181Committee [8, Appendix 2]

Appendix 2

VEHICLE TITLE FS E444 LOCOMOTIVE

MASSES & INERTIAS

Number of bogies	2
Number of axles (per bogie)	2
Body mass	64.6 Mg
Body roll inertia	53.366 Mgm ²
Body pitch inertia	1643.0 Mgm ²
Body yaw inertia	1630.0 Mgm ²
Bogie mass	4.0 Mg
Bogie roll inertia	3.115 Mgm ²
Bogie pitch inertia	5.843 Mgm ²
Bogie yaw inertia	8.107 Mgm ²
Wheelset mass	2.1 Mg
Wheelset roll and yaw inertia	1.164 Mgm ²

DIMENSIONS

Semi pivot spacing	4.5 m
Semi wheelbase	1.3 m
Wheel radius	0.55 m
Body centre of gravity height above rail level	1.65 m
Bogie centre of gravity height above rail level	0.64 m

PRIMARY SUSPENSION

Lateral stiffness (per axle)	12.0 MN/m
Vertical stiffness (per axle)	4.0 MN/m
Yaw stiffness (per axle)	15.4 MNm/r
Lateral damper rate (per axle)	- MNs/m
Vertical damper rate (per axle)	0.03 MNs/m
Vertical friction breakout (per axle)	- KN
Height above rail level of lateral springs	0.55 m
Lateral semi spacing of vertical springs	1.03 m
Height above rail level of lateral dampers	- m
Lateral semi spacing of vertical dampers	1.2 m
Lateral semi spacing of vertical friction	- m

958223/01

9

Figure C.9: FS E444 LOCOMOTIVE. Extract from D181Committee [8, Appendix 2]

Appendix 2

SECONDARY SUSPENSION

Lateral stiffness (per bogie)	1.0 MN/m
Vertical stiffness (per bogie)	2.1 N/m
Roll bar stiffness (per bogie)	1.0 Nm/r
Yaw stiffness (per bogie)	- Nm/r
Lateral damper rate (per bogie)	0.037 MNs/m
Vertical damper rate (per bogie)	0.145 MNs/m
Yaw damper rate (per bogie)	0.938 MNms/r
Height above rail level of lateral springs	0.95 m
Lateral semi spacing of vertical springs	1.03 m
Height above rail level of lateral dampers	0.73 m
Lateral semi spacing of vertical dampers	1.20 m

Figure C.10: FS E444 LOCOMOTIVE. Extract from D181Committee [8, Appendix 2]

Appendix 2

VEHICLE TITLE UIC COACH

MASSES & INERTIAS

Number of bogies	2
Number of axles (per bogie)	2
Body mass	32.0 Mg
Body roll inertia	56.8 Mgm ²
Body pitch inertia	1970.0 Mgm ²
Body yaw inertia	1970.0 Mgm ²
Bogie mass	2.615 Mg
Bogie roll inertia	1.722 Mgm ²
Bogie pitch inertia	1.476 Mgm ²
Bogie yaw inertia	3.067 Mgm ²
Wheelset mass	1.70 Mg
Wheelset roll and yaw inertia	1.30 Mgm ²

DIMENSIONS

Semi pivot spacing	9.5 m
Semi wheelbase	1.28 m
Wheel radius	0.445 m
Body centre of gravity height above rail level	1.503 m
Bogie centre of gravity height above rail level	0.68 m

PRIMARY SUSPENSION

Lateral stiffness (per axle)	6.4 MN/m
Vertical stiffness (per axle)	1.46 MN/m
Yaw stiffness (per axle)	60.0 MNm/r
Lateral damper rate (per axle)	- MNs/m
Vertical damper rate (per axle)	0.005 MNs/m
Vertical friction breakout (per axle)	- KN
Height above rail level of lateral springs	0.445 m
Lateral semi spacing of vertical springs	1.0 m
Height above rail level of lateral dampers	- m
Lateral semi spacing of vertical dampers	1.0 m
Lateral semi spacing of vertical friction	- m

958223/01

11

Figure C.11: UIC COACH. Extract from D181Committee [8, Appendix 2]

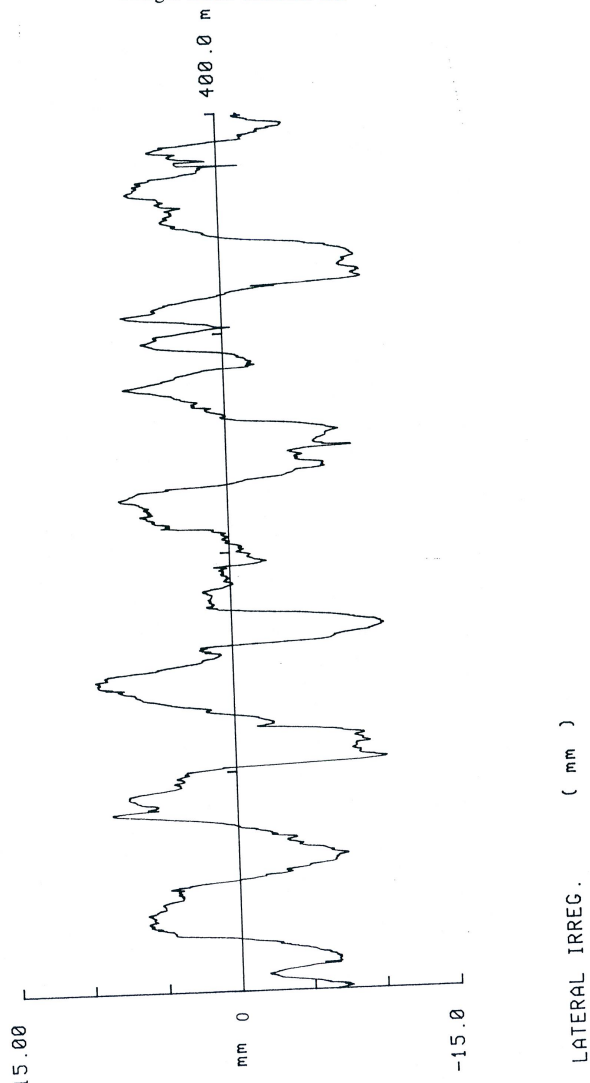
Appendix 2

SECONDARY SUSPENSION

Lateral stiffness (per bogie)	0.32 MN/m
Vertical stiffness (per bogie)	0.86 MN/m
Roll bar stiffness (per bogie)	0.94 MNm/r
Yaw stiffness (per bogie)	- MNm/r
Lateral damper rate (per bogie)	0.059 MNs/m
Vertical damper rate (per bogie)	0.074 MNs/m
Yaw damper rate (per bogie)	0.591 MNms/r
Height above rail level of lateral springs	0.825 m
Lateral semi spacing of vertical springs	1.0 m
Height above rail level of lateral dampers	0.825 m
Lateral semi spacing of vertical dampers	1.3 m

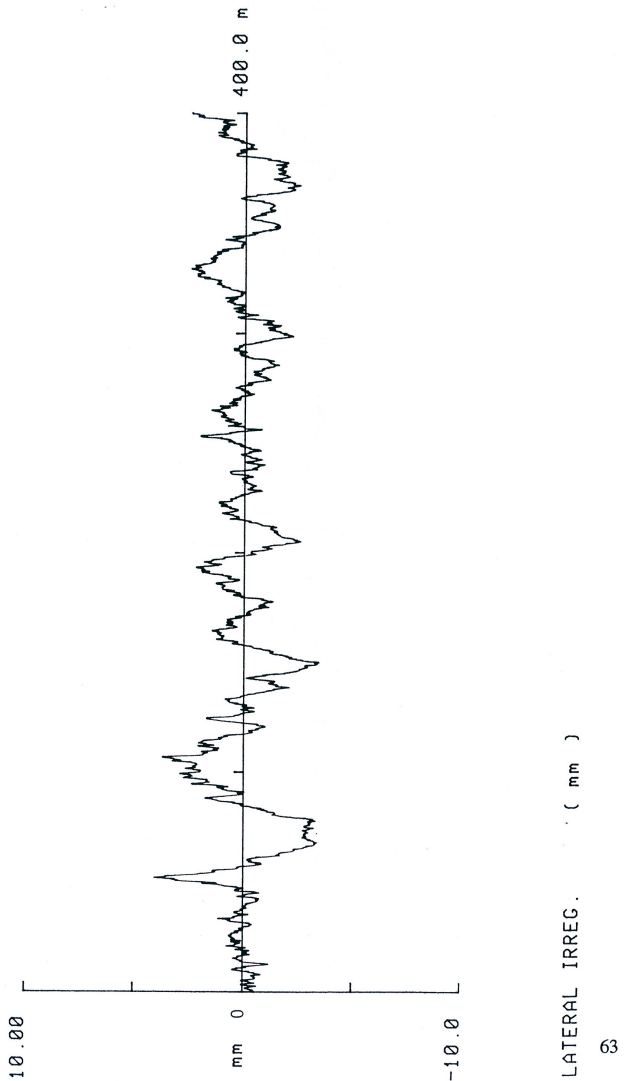
Figure C.12: UIC COACH. Extract from D181Committee [8, Appendix 2]

Freight track: Trackfrt. dat



ERRI D 181/RP 6	VAMPIRE HORIZONTAL TRACK IRREGULARITIES (PASSENGER)	Fig. 2.2
-----------------	--	----------

Passenger track: Trackpn. dat



63

Figure C.14: Horizontal track irregularities for standard passenger trains. Extract from D181Committee [7, Figure 2.1]

ERRI D 181/RP 6	VAMPIRE HORIZONTAL TRACK IRREGULARITIES (HIGH-SPEED LINE)	Fig. 2.3
-----------------	---	----------

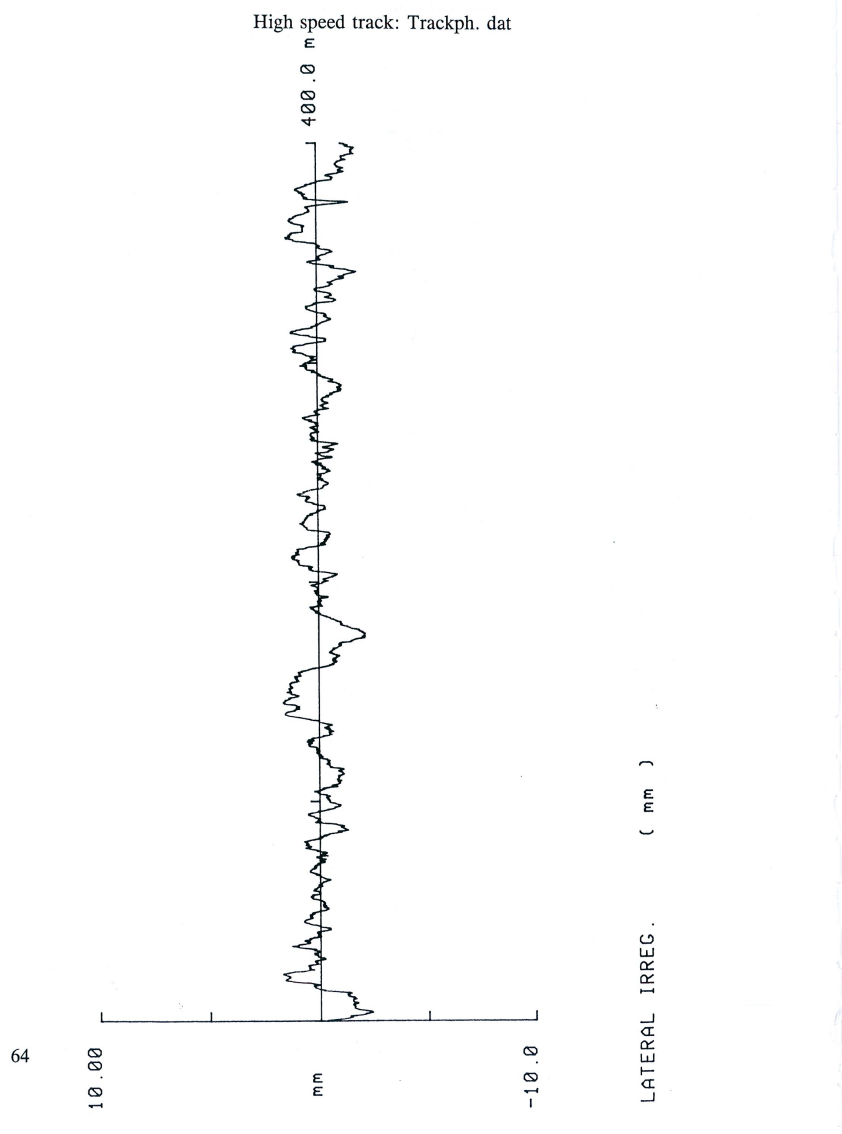


Figure C.15: Horizontal track irregularities for high speed passenger train. Extract from D181Committee [7, Figure 2.1]

Appendix D

**Speeds which do not
require dynamic
compatibility checks**

Line category Locomotive class	Freight wagon	Locomotive	Passenger carriage	Multiple unit	Special vehicle
a10 ^a	-	-	-	-	-
a12 ^a	-	-	-	-	-
a14 ^a	-	-	-	-	-
A	120	120 ^b / 160	160 ^c	160 ^c	120
B1	120	120 ^b / 160	160 ^c	160 ^c	120
B2	120	120 ^b / 160	-	-	120
C2	120	120 ^b / 160	140 ^c	140 ^c	120
C3	120	120	-	-	120
C4	120	120	-	-	120
D2	120	120 ^b / 160	120 ^c	120 ^c	120
D3	120	120	-	-	120
D4	120	120	-	-	120
D4xL	120 ^d	120	-	-	120 ^d
D5	100	-	-	-	100
E4	100	-	-	-	100
E5	100	-	-	-	100
E6	80	-	-	-	80
L4	-	120 ^b / 160	-	-	-
L6	-	120	-	-	-

^a Light railways – normal operating speeds are generally significantly less than speed at which additional dynamic checks would need to be considered.
^b Three or more adjacent couples locomotives.
^c Additional values for max "p" (see Table F.2).
^d Option.

Figure D.1: Speed limit (in km/h) in relationship Line Category/Locomotive Class and vehicle type. Extract from CEN [6, Appendix F]

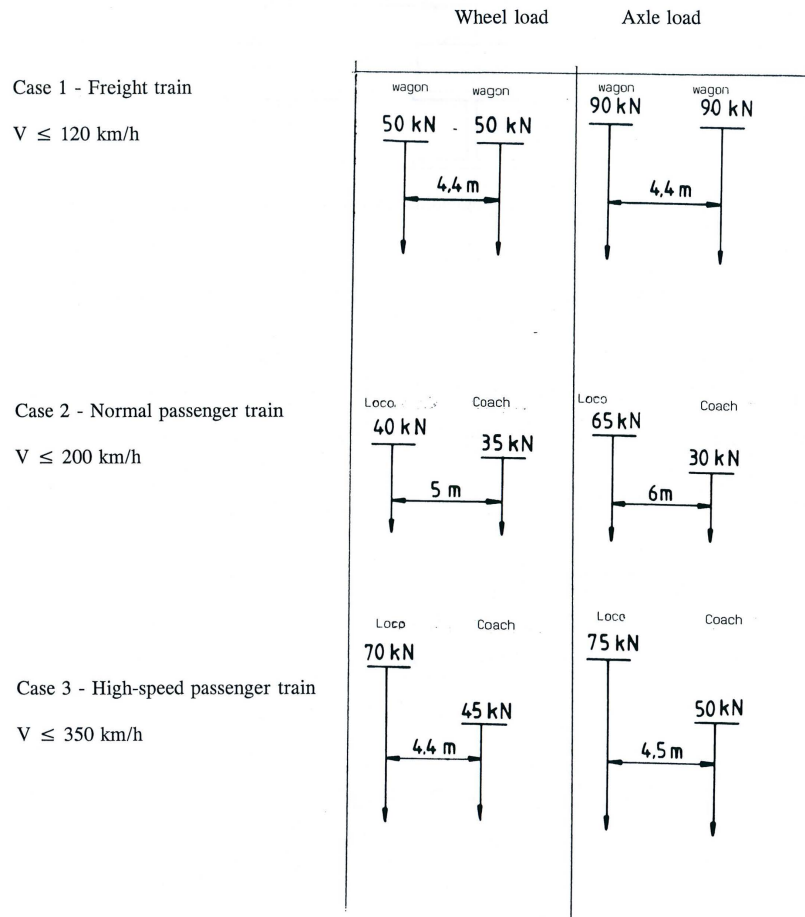


Figure D.2: LATERAL WHEEL AND AXLE FORCES FOR BRIDGES. Extract from D181Committee [7, Fig 3.1]

EXAMPLE RUN FILE

```

Case 7: Passenger train/track, 160kph, 54m span, 1/10000 flex., 6 Mg/m
EUROLONG
*TRANSIENT
    470  0.0010  0.01
    44.44

trackPN
*CREEP
    0.3000  0.3000  8.0000  0.0000  0.0000
NO-NLINEAR
skip1
*OUTPUT
Lat displacement of bridge @ mid span mm
1000*1001
Lat acceleration of bridge @ mid span m/s2
U02
LOCO body lat accel @ leading pivot m/s2
A01Y + 4.5*A01W
COACH 1 body lat accel @ leading pivot m/s2
A02Y + 9.5*A08W
LOCO lat accel of leading bogie m/s2
A02Y
COACH 1 lat accel of leading bogie m/s2
A09Y
Total lat force on LOCO leading bogie kN
FW01Y + FW02Y
Total lat force on COACH 1 leading bogie kN
FW05Y + FW06Y
Lat force, COACH 1 wset 1, left wheel kN
Lat force, COACH 1 wset 1, right wheel kN
FR03Y
Lat force, COACH 1 wset 2, left wheel kN
FR06Y
Lat force, LOCO wset 1, left wheel kN
FL01Y
Lat force, LOCO wset 1, right wheel kN
FR01Y
Lat force, LOCO wset 2, left wheel kN
FL02Y
Lat force, LOCO wset 2, right wheel kN
FL03Y
Lat force, LOCO wset 3, left wheel kN
FL04Y
Lat force, LOCO wset 3, right wheel kN
FR05Y
COACH 5 body lat accel @ leading pivot m/s2
A36Y + 9.5*A36W
COACH 5 lat accel of leading bogie m/s2
A37Y
Total lat force on COACH 5 leading bogie kN
FW21Y + FW22Y
Lat force, COACH 5 wset 1, left wheel kN
FL21Y
Lat force, COACH 5 wset 1, right wheel kN
FR21Y
Lat force, COACH 5 wset 2, left wheel kN
FL22Y
Lat force, COACH 5 wset 2, right wheel kN
FR22Y
*

```

958223/01

Figure D.3: Example run file. Extracted from D181Committee [8].

Appendix E

MU-Groups and MU-Classes

E.1 Definition

Multiple units can be grouped according to type of traffic service (high speed - long distance, intercity - regional and commuter/suburban) or to the kind of running gear (conventional bogies, articulated bogies and single axles).

In some cases due to potential excessive dynamic load effects in bridge line category checks are not sufficient to demonstrate compatibility. To minimise the need for undertaking a dynamic check of individual trains, several typical and wide spread MU-designs have been grouped in MU-classes. For these groups of vehicles, load models covering the specified design parameter ranges have been developed to allow the efficient dynamic analysis of bridges. For practical reasons, the number of MU classes was limited and for trains outside the range of parameters covered, the process of checking an individual train existing at the time of publication of this standard as state of the art shall be used.

Each MU-class is defined by:

- ranges of train parameters covered and;
- a corresponding load model for carrying out dynamic checks on bridges.

Each MU-Group comprises of several MU-Classes. Table

MU-Group	MU-Class
conventional bogie(CB)	CB_1 CB_2
articulated bogie(AB)	AB_1 AB_2 AB_3 AB_4
single axle(SA)	SA_1 SA_2

Table E.1: Relationship MU-groups - MU-classes

Name	Parameter	Unit
$2a^*$	Bogie spacing between pivot centres within a vehicle	m
$2a^+$	Axle spacing in bogie	m
$u1 + u2$	Bogie spacing between pivot centres of adjacent vehicles	m
$u3$	Overhang of end coaches	m
L_Coa	Coach length	m
No_Coa	Number of coaches within an unit	-
No_Units	Number of units within a train	-

Table E.2: Explanation of train parameters. Extracted from CEN [6, Annex C]

- E.1.1 Train parameters of MU-Class CB_1
- E.1.2 Train parameters of MU-Class CB_2
- E.1.3 Train parameters of MU-Class AB_1
- E.1.4 Train parameters of MU-Class AB_2
- E.1.5 Train parameters of MU-Class AB_3
- E.1.6 Train parameters of MU-Class AB_4
- E.1.7 Train parameters of MU-Class SA_1
- E.1.8 Train parameters of MU-Class SA_2

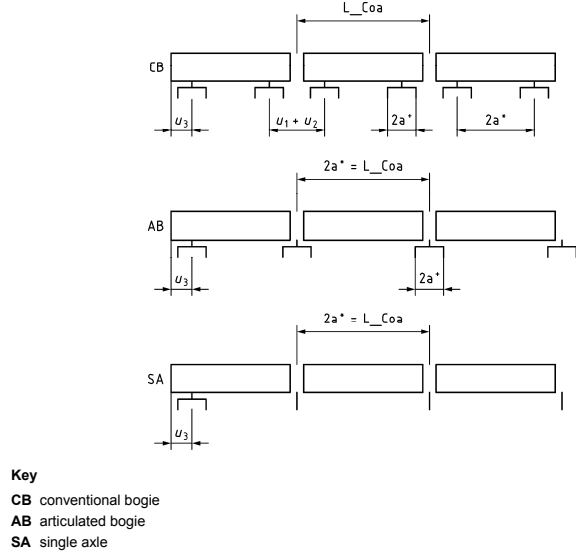


Figure E.1: Train parameters related to MU-Groups. Extracted from CEN [6, Annex C]

max No_Units	2
max No_Coa	8
L_Coa	$23.8m \leq L_{Coa} \leq 25.3m$
$2a^*$	$16.8m \leq 2a^* \leq 18.0m$
$2a^+$	$2m \leq 2a^+ \leq 3m$
$(u1 + u2)$	$7.0m \leq (u1 + u2) \leq 7.6m$
$u3$	$4m \leq u3 \leq 6m$

Table E.3: Train parameters for conformity with MU-Class CB_1

max No_Units	2
max No_Coa	7
L_Coa	$25.3m \leq L_{Coa} \leq 27.5m$
$2a^*$	$18.0m \leq 2a^* \leq 19.5m$
$2a^+$	$2m \leq 2a^+ \leq 3m$
$(u1 + u2)$	$7.2m \leq (u1 + u2) \leq 8.0m$
$u3$	$4m \leq u3 \leq 6m$

Table E.4: Train parameters for conformity with MU-Class CB_2

max No_Units	4
max No_Coa	5
$2a^*$	$14.9m \leq 2a^* \leq 16.0m$
$2a^+$	$2m \leq 2a^+ \leq 3m$
$u3$	$3m \leq u3 \leq 5.5m$

Table E.5: Train parameters for conformity with MU-Class AB_1

max No_Units	4
max No_Coa	5
$2a^*$	$18.8m \leq 2a^* \leq 19.5m$
$2a^+$	$2m \leq 2a^+ \leq 3m$
$u3$	$3m \leq u3 \leq 5.5m$

Table E.6: Train parameters for conformity with MU-Class AB_2

max No_Units	2
max No_Coa	11
$2a^*$	$17.0m \leq 2a^* \leq 17.5m$
$2a^+$	$2m \leq 2a^+ \leq 3m$
$u3$	$4.5m \leq u3 \leq 5.7m$

Table E.7: Train parameters for conformity with MU-Class AB_3

max No_Units	2
max No_Coa	10
$2a^*$	$18.7m \leq 2a^* \leq 19.2m$
$2a^+$	$2m \leq 2a^+ \leq 3m$
$u3$	$4.3m \leq u3 \leq 5.3m$

Table E.8: Train parameters for conformity with MU-Class AB_4

max No_Units	3
max No_Coa	10
$2a^*$	$9.2m \leq 2a^* \leq 9.8m$
$u3$	$4.25m \leq u3 \leq 6.25m$

Table E.9: Train parameters for conformity with MU-Class SA_1

max No_Units	2
max No_Coa	14
$2a^*$	$12.8m \leq 2a^* \leq 13.5m$
$u3$	$4.25m \leq u3 \leq 6.25m$

Table E.10: Train parameters for conformity with MU-Class SA_2

Appendix F

Regression commands for R console

```
> F < c(0,110,170,185)
> v < c(0,60,100,120)
> f < function(a,b,v) {a*v^b}
> dat < data.frame(v,F)
> dat
   v     F
1 0    0
2 60   110
3 100  170
4 120  185

> fm < nls(F ~ f(a,b,v), data = dat, start = c(a=1, b=1))
> fm
Nonlinear regression model
  model: F ~ f(a, b, v)
  data: dat
      a      b
 5.2064 0.7498
 residual sum of squares: 47.84

Number of iterations to convergence: 6
Achieved convergence tolerance: 2.868e-06
```

Appendix G

Matlab scripts

G.1 fog.m

```
% This script is the main utility to function automated  
% bridge lateral dynamic response evaluation  
  
function O=fog(EJ,l,mu,c,zeta)  
  
if EJ<1  
    EJ = 100000*l^2/(48*EJ);  
end  
  
omegal = pi^2/l^2*sqrt(EJ/mu);  
omega = pi*c/l;  
omegab = zeta*sqrt(EJ/mu);  
omegab = 0.5*zeta*omegal;  
% omegab = omegal*sqrt(1 zeta ^2)  
omegal1 = sqrt(abs(omegal^2 omegab^2));  
Omega = 2*pi*c/10;  
  
r1 = Omega + omega;  
r2 = Omega - omega;  
  
% if c >= (200/3.6)  
%     Q = 3.10*(c*3.6)^0.7495;  
% end  
%  
% if c >= (120/3.6) && c < (200/3.6)
```

```

%      Q = 3.58*(c*3.6) ^0.7495;
% end
%
% if c < (120/3.6)
%      Q = 5.2064*(c*3.6) ^0.7495;
% end

% Q = Q;
% Q = 10000
Q = 1928*c ^0.7495;
f = omega1/(2*pi);
v_0 = Q*1^3/(48*EJ);
%omegab = 0.0001*sqrt(EJ/mu);

beta = omegab/omega1;

v1 = @(t) 1^3*Q*omega1/(pi^4*EJ) * cos(omega1*t)/(omega
^2+omegab^2);
v2 = @(t) omega*(cos(omega*t) exp(-omegab*t)) omegab*sin(
omega*t);
v = @(t) v1(t) * v2(t);

% v11 = 1/((omega1^2 r2^2)^2+4*omegab^2*r2^2);
% v12 = @(t) (omega1^2 r2^2)*(cos(r2*t) exp(-omegab*t)*
cos(omega1*a*t));
% v13 = @(t) 2*omegab*r2*sin(r2*t);
% v14 = @(t) omegab/omega1*a*(omega1^2+r2^2)*exp(-omegab*
t)*sin(omega1*a*t);
% v21 = 1/((omega1^2 r1^2)^2+4*omegab^2*r1^2);
% v22 = @(t) (omega1^2 r1^2)*(cos(r1*t) exp(-omegab*t)*
cos(omega1*a*t));
% v23 = @(t) 2*omegab*r1*sin(r1*t);
% v24 = @(t) omegab/omega1*a*(omega1^2+r1^2)*exp(-omegab*
t)*sin(omega1*a*t);
% v = @(t) Q/(mu*1)*(v11*(v12(t)+v13(t)+v14(t))+v21*(v22(
t)+v23(t)+v24(t)));

a11 = @(t) 1^3*Q*omega1^3*cos(omega1*t)/(pi^4*EJ*(omega
^2+omegab^2));
a12 = @(t) omega*(cos(omega*t) exp(-omegab*t)) omegab*sin(
omega*t);
a21 = @(t) 1^3*Q*omega1*cos(omega1*t)/(pi^4*EJ*(omega^2+
omegab^2));

```

```

a221 = @(t) omega*( cos(omega*t)*omega^2*exp(-omegab*t)*
    omegab^2);
a222 = @(t) omegab*sin(omega*t)*omega^2;
a22 = @(t) a221(t)+a222(t);
a31 = @(t) 2*l^3*Q*omega1^2*sin(omegal*t)/(pi^4*EJ*( 
    omega^2+omegab^2));
a32 = @(t) omega*( sin(omega*t)+exp(-omegab*t)*omegab)
    omegab*cos(omega*t)*omega;
a = @(t) a11(t)*a12(t)+a21(t)*a22(t)+a31(t)*a32(t);

maxt = 1/c;
dt = maxt/1000;
tdomain = [0:dt:maxt]';

for i=1:length(tdomain)
    p(i,1) = v(tdomain(i,1));
    p(i,2) = a(tdomain(i,1));
    p(i,3) = p(i,1)/v_0;
end

O = [max(abs(p(:,1))),max(abs(p(:,2))),max(abs(p(:,3)))];

namedef = strcat('EJ',int2str(EJ),'L',int2str(l),'mu',
    int2str(mu),'c',int2str(c),'daf','.tikz');
%%%
%% figure(1)
% plot(tdomain,p(:,1),linecolor)
% grid on
% title(strcat('Max Deflection:',mat2str(O(1,1))));
%% matlab2tikz(namedef,'height','\figureheight',
% width','\figurewidth','showInfo',false);
%%%
%% figure(2)
% plot(tdomain,p(:,2))
% grid on
% title(strcat('Max Acceleration:',mat2str(O(1,2))));
%% matlab2tikz(nameacc,'height','\figureheight',
% width','\figurewidth','showInfo',false);
%%%
%% figure(3)
% plot(tdomain,p(:,3))
% grid on
% title(strcat('Max Deflection:',mat2str(O(1,1)),',Max
% Acceleration:',mat2str(O(1,2))));
% matlab2tikz(namedaf,'height','\figureheight',
% width'

```

```
', '\figurewidth', 'showInfo', false);
```

G.2 Speedenvelop.m

```
function O=Speedenvelop(EJ,l,mu,min,max,zeta)

dv = 0.2;
v = [min:dv:max]';

for i=1:length(v)
    maxres(:,i) = fog(EJ,l,mu,v(i,1),zeta,'b');
    speed = v(i,1);
end

% figure('name','speed_envelop');
% plot(v,maxres);

namedef = strcat('speedef','EJ',int2str(EJ),'L',int2str(l),
                  ',min',int2str(min),',max',int2str(max),',mu',int2str(mu),
                  ',.tikz')
nameacc = strcat('speacc','EJ',int2str(EJ),'L',int2str(l),
                  ',min',int2str(min),',max',int2str(max),',mu',int2str(mu),
                  ',.tikz')
nameaco = strcat('speaco','EJ',int2str(EJ),'L',int2str(l),
                  ',min',int2str(min),',max',int2str(max),',mu',int2str(mu),
                  ',.tikz')

figure(1)
plot(v,maxres(1,:))
title(strcat('SpeedEnvelop def from',int2str(min),', to ',
            int2str(max)));
matlab2tikz(namedef, 'height', '\figureheight', 'width',
             '\figurewidth', 'showInfo', false);

figure(2)
plot(v,maxres(2,:))
title(strcat('SpeedEnvelop acc from',int2str(min),', to ',
            int2str(max)));
%matlab2tikz(nameacc, 'height', '\figureheight', 'width',
%             '\figurewidth', 'showInfo', false);

figure(3)
plot(v,maxres(3,:))
```

```
title(strcat('SpeedEnvelop dc from', int2str(min), ' to ',
    int2str(max)));
%matlab2tikz(nameaco, 'height', '\figureheight', 'width',
'\figurewidth', 'showInfo', false);
```

Appendix H

Train vehicles

H.1 Locomotives

H.1.1 4-axle locomotives

Generally, the relevant parameters for categorisation of 4-axle locomotives are axle load P (18 t to 22,5 t) and the bogie axle spacing (2,2 m to 3,4 m).

Typically the mass per unit length is less than 6,4 t/m and the distance from the end axle to the end of the nearest coupling plane is greater than 1,9 m

H.1.2 6-axle locomotives

Generally, the relevant parameters for categorisation of 6-axle locomotives are:

- the maximum axle load P (18 t to 22 t) in combination with;
- the distance between axles within a bogie (1,80 m to 2,25 m).

Typically, the mass per unit length (p) is less than 6,4 t/m and the distance from end axle to the end of the nearest coupling plane (a) is greater than 2,1 m.

H.2 Trains in Netherlands

Passenger trains now in service include following models:

1. The DD-AR (Dubbeldeksaggloregiomaterieel)
EMUs were delivered as DDM-2/3 resembling the bilevel rail cars series

DDM-1 from 1985 and operates in fixed formations of 3 or 4 coaches. 4 car trains use a class 1700 locomotive for traction, 3 car trains use an mDDM motorcar, which resembles a DD-AR driving trailer but has electric motors and a single passenger deck on top; the level of this deck is higher than that of a regular single deck rail car, but lower than the upper deck of the other coaches. Three types of coaches are available: Bv (second class), ABv (first and second class) and Bvk (second class driving trailer). The DDM-2/3 series are being modernised from 2010/2013 and after modernisation the series was renamed as NID (Nieuwe Intercity Dubbeldekker).

2. The VIRM (Verlengd Interregiomaterieel)

also called Regiorunner was partially rebuilt from trainsets DD-IRM (Dubbeldeks Interregiomaterieel). DD-IRM was delivered in 3- and 4-car trainsets. 3-car trainsets got one extra coach, 4-car trainsets got two extra coaches. Also, new 4- and 6-car trainsets were built. Thus, a train consists of one or more combinations of 4 or 6 double deck coaches; each combination (multiple unit) has electric motors. More than three hundred coaches are currently operative in the Netherlands.

3. The Koploper (ICM) (Intercitymaterieel)

is a 3- or 4-car multiple unit that when coupled with another one, allows passengers to walk through (the name Koploper being a play on words literally "head walker", but in actual use meaning "front runner"). The Dutch Railway Company decided to close the heads permanently on 31 October 2005 because the mechanism broke down too often. A scheduled modernisation of around 7 million euro will see the ICM fleet updated. The renovated ICM trains provide 13% more seats (reducing the leg room to uncomfortable small for the long haul journeys they serve in 2nd class, which is further aggravated by a waste bin that is placed on the back-sides of the seats in front), have a new interior, a bathroom accessible by wheelchairs, airconditioning as well as upgrades to the engine and connection systems. The head doors are removed. Also, these (renovated) trains are the first trains in the NS fleet equipped with OBIS. OBIS provides a (free) WiFi-connection on board, along with in-train journey information provided through screens and (automated) vocal announcements through the trains speakers. This journey information provides the actual status, and thus is always up-to-date to the actual situation this trip, and the stations is passes.

4. The Sprinter (SGM, Stads Gewestelijk Materieel)

is a two or three car electric, used on small distances. They are named Sprinter because they're able to accelerate and brake quite fast, making them very suitable for 'stoptrein' services. They were also specifically designed for urban environments where they run commuter services. As a result, they are most commonly found in the Randstad area. The initial idea was that the Sprinter would provide somewhat of a subway/metro service but this plan failed as the cities of Amsterdam and Rotterdam

continued to construct their own rapid transit systems. Nevertheless, in the densely populated Randstad, the Sprinters remain popular. Two car versions were revised and renamed to Citypendel. All Sprinters are now refurbished into the new white/yellow/dark blue livery.

Bibliography

- [1] EN 1990 AMD 2 : 2005(E) Annex A2 to EN 1990.
- [2] M Abu-Hilal and M Mohsen. Vibration of beams with general boundary conditions due to a moving harmonic load. *Journal of Sound and Vibration*, 232(4):703–717, 2000.
- [3] CEN. EN 13848-5:2008+A1 Railway applications - Track - Track geometry quality - Part 5: Geometric quality levels - Plain line.
- [4] CEN. 1: Actions on structures, part 2: Traffic loads on bridges. *Brussels: European Standard EN*, 2:2003, 1991.
- [5] CEN. *Eurocode: Basis of structural design*. BSI, 2002.
- [6] CEN. pren 15528:2013, railway applications line categories for managing the interface between load limits of vehicles and infrastructure. *Brussels: European Standard EN*, 2013.
- [7] D181Committee. *RP6: Final report, D181 LATERAL FORCES ON RAILWAY BRIDGES*. UIC, .
- [8] D181Committee. *ERRI D 181/DT 329 E: LATERAL FORCES ON RAILWAY BRIDGES, PARAMETRIC STUDY PART1,PART 2*. UIC, .
- [9] Coenraad Esved. Modern railway track. 2001.
- [10] Ladislav Frýba. *Vibration of solids and structures under moving loads*. Thomas Telford, 1999.
- [11] JJ Reber. Presentation on lateral stiffness of railway bridges. 2013.
- [12] UIC. *UIC Leaflet 776-2:Design requirements for rail-bridges based on interaction phenomena between train, track and bridge*. UIC, June 2009.